

AD-A240 656



2

NAVAL POSTGRADUATE SCHOOL  
Monterey, California



DTIC  
ELECTE  
SEP 23 1991  
S B D

THESIS

DISCRETE ARMA MODEL FOR NATURAL  
RESONANCES IN ELECTROMAGNETIC AND  
ACOUSTIC SCATTERING

by

Yuval Cohen

September 1990

Thesis Advisor:

Michael A. Morgan

Approved for public release; distribution is unlimited.

91-11222

01 9 20 024

UNCLASSIFIED

SECURITY CLASSIFICATION OF THIS PAGE

REPORT DOCUMENTATION PAGE				Form Approved OMB No. 0704-0188	
1a REPORT SECURITY CLASSIFICATION UNCLASSIFIED			1b RESTRICTIVE MARKINGS		
2a SECURITY CLASSIFICATION AUTHORITY			3 DISTRIBUTION/AVAILABILITY OF REPORT Approved for public release; distribution is unlimited		
2b. DECLASSIFICATION/DOWNGRADING SCHEDULE					
4 PERFORMING ORGANIZATION REPORT NUMBER(S)			5. MONITORING ORGANIZATION REPORT NUMBER(S)		
6a NAME OF PERFORMING ORGANIZATION Naval Postgraduate School		6b OFFICE SYMBOL (If applicable) EC	7a. NAME OF MONITORING ORGANIZATION Naval Postgraduate School		
6c. ADDRESS (City, State, and ZIP Code) Monterey, CA 93943-5000			7b. ADDRESS (City, State, and ZIP Code) Monterey, CA 93943-5000		
8a NAME OF FUNDING SPONSORING ORGANIZATION		8b. OFFICE SYMBOL (If applicable)	9 PROCUREMENT INSTRUMENT IDENTIFICATION NUMBER		
8c. ADDRESS (City, State, and ZIP Code)			10 SOURCE OF FUNDING NUMBERS		
			PROGRAM ELEMENT NO	PROJECT NO	TASK NO
			WORK UNIT ACCESSION NO.		
11 TITLE (Include Security Classification) DISCRETE ARMA MODEL FOR NATURAL RESONANCES IN ELECTROMAGNETIC AND ACOUSTIC SCATTERING					
12 PERSONAL AUTHOR(S) COHEN, Yuval					
13a TYPE OF REPORT Master's Thesis		13b TIME COVERED FROM _____ TO _____		14 DATE OF REPORT (Year, Month, Day) 1990 September	
15 PAGE COUNT 95					
16 SUPPLEMENTARY NOTATION The views expressed in this thesis are those of the author and do not reflect the official policy or position of the Depart- ment of Defense or the US Government.					
17 COSATI CODES			18 SUBJECT TERMS (Continue on reverse if necessary and identify by block number)		
FIELD	GROUP	SUB-GROUP	Natural Resonances; Electromagnetic Scattering; Acoustic Scattering; Radar Target Identifica- tion; Prony's Method; ARMA Model		
19 ABSTRACT (Continue on reverse if necessary and identify by block number) Investigations of scattered transient waveforms from conducting bodies have shown that it is possible to classify electromagnetic scatterers. The con- cept is based upon the natural resonance modes which are part of the scat- terer response to an incident excitation. A new approach for describing natural resonance modes using recursive systems is introduced. A discrete auto-regressive moving-average (ARMA) type model for the case of the space- time wave equation is presented. This model results from a finite-differ- ence approximation to the wave-equation. The ARMA model has spatially- independent coefficients for the temporal recursive terms. Computed results showing aspect- and spatial-independence of natural resonance modes, with verification of the ARMA model, are also included. Applica- tions to target identification, using the natural resonant frequencies of the target's echo signature, are considered.					
20 DISTRIBUTION/AVAILABILITY OF ABSTRACT <input checked="" type="checkbox"/> UNCLASSIFIED/UNLIMITED <input type="checkbox"/> SAME AS RPT <input type="checkbox"/> DTIC USERS			21 ABSTRACT SECURITY CLASSIFICATION UNCLASSIFIED		
22a NAME OF RESPONSIBLE INDIVIDUAL MORGAN, Michael A.			22b TELEPHONE (Include Area Code) 408-646-2082		22c OFFICE SYMBOL EC

DD Form 1473, JUN 86

Previous editions are obsolete

S/N 0102-LF-014-6603

SECURITY CLASSIFICATION OF THIS PAGE

UNCLASSIFIED

Approved for public release; distribution is unlimited.

Discrete ARMA Model for Natural Resonances  
in Electromagnetic and Acoustic Scattering

by

Yuval Cohen

Lieutenant Commander, Israeli Navy  
B.Sc. in Electrical Engineering, Technion-Israel  
Institute of Technology, Haifa, Israel, 1986

Submitted in partial fulfillment  
of the requirements for the degree of

MASTER OF SCIENCE IN ELECTRICAL ENGINEERING

from the

NAVAL POSTGRADUATE SCHOOL

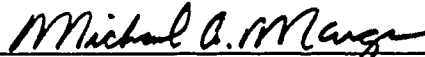
September 1990

Author:



Yuval Cohen

Approved by:



Michael A. Morgan, Thesis Advisor



Richard W. Adler, Second Reader



Michael A. Morgan, Chairman

Department of Electrical and Computer Engineering

## ABSTRACT

Investigations of scattered transient waveforms from conducting bodies have shown that it is possible to classify electromagnetic scatterers. The concept is based upon the natural resonance modes which are part of the scatterer response to an incident excitation. A new approach for describing natural resonance modes using recursive systems is introduced. A discrete auto-regressive moving-average (ARMA) type model for the case of the space-time wave equation is presented. This model results from a finite-difference approximation to the wave-equation. The ARMA model has spatially-independent coefficients for the temporal recursive terms. Computed results showing aspect- and spatial-independence of natural resonance modes, with verification of the ARMA model, are also included. Applications to target identification, using the natural resonant frequencies of the target's echo signature, are considered.



Accession For	
NTIS GRA&I	<input checked="" type="checkbox"/>
DTIC TAB	<input type="checkbox"/>
Unannounced	<input type="checkbox"/>
Justification _____	
By _____	
Distribution/	
Availability Codes	
Dist	Avail and/or Special
A-1	

## TABLE OF CONTENTS

I. INTRODUCTION .....	1
A. BACKGROUND .....	1
B. PRESENTATION IN A DISCRETE MODEL .....	2
C. THESIS GOAL .....	3
II. THE THEORY OF NATURAL RESONANCE SCATTERING .....	5
A. INTRODUCTION .....	5
B. TIME DOMAIN INTEGRAL EQUATIONS .....	6
C. NATURAL RESONANCE SCATTERING .....	11
D. THIN WIRE CASE .....	14
E. SUMMARY .....	16
III. ELECTROMAGNETIC AND ACOUSTIC SCATTERING	
EXAMPLES .....	18
A. INTRODUCTION .....	18
B. DERIVATION OF THE VECTOR POTENTIAL EQUATION ..	19
C. VIBRATING STRING WITH FORCING FUNCTION .....	22

D. FINITE-DIFFERENCE APPROXIMATION TO THE WAVE EQUATION .....	25
E. NUMERICAL CONSIDERATIONS .....	28
F. COMPUTED RESULTS .....	30
IV. THE DISCRETE ARMA MODEL .....	43
A. INTRODUCTION .....	43
B. THE PROBLEM .....	45
C. ANALYTICAL SOLUTION FOR RESONANCE MODES .....	47
D. NUMERICAL SOLUTION FOR RESONANCE MODES: LOSSLESS CASE .....	50
E. NUMERICAL SOLUTION FOR RESONANCE MODES: LOSSY CASE .....	53
F. ARMA MODEL DEVELOPMENT .....	54
G. VALIDATION EXAMPLE: LOSSLESS CASE .....	55
H. VALIDATION EXAMPLE: LOSSY CASE .....	60
I. COMPUTED RESULTS .....	62
VI. CONCLUSIONS .....	65
APPENDIX A. SPACE-TIME WAVE EQUATION PROGRAM .....	67

APPENDIX B. ARMA MODEL ALGORITHM .....	77
APPENDIX C. PRONY'S METHOD PROGRAM .....	79
LIST OF REFERENCES .....	81
INITIAL DISTRIBUTION LIST .....	83

## LIST OF FIGURES

Figure 1. Transient Electromagnetic Scattering [After Ref. 4] .....	6
Figure 2. Region of Interaction .....	10
Figure 3. Short Pulse Wave Illumination. [After Ref. 4] .....	12
Figure 4. Geometry of a Cylindrical Thin Wire Scatterer .....	14
Figure 5. Characteristics [From Ref. 11] .....	24
Figure 6. Multiple Reflected Characteristics. [From Ref. 11] .....	24
Figure 7. Space-Time Discretization .....	26
Figure 8. Star Operator .....	27
Figure 9. Gaussian Pulse Excitation .....	31
Figure 10. String Displacement for Broadside Excitation .....	33
Figure 11. Displacement of Segments 2 and 8 (Lossy Case) .....	34
Figure 12. String Displacement for 30 Degree Incident Angle .....	35
Figure 13. Resonant Frequencies (30 Degrees) .....	37
Figure 14. Modes of All Segments (30 Degrees) .....	38
Figure 15. Modes of All Segments (Broadside) .....	39
Figure 16. Modes on Segment 22 .....	41
Figure 17. Modes on Segment 6 .....	42
Figure 18. Realization of the General Model [After Ref. 5] .....	46



Figure 19. Space-Time Discretization for Mode Solution .....	51
Figure 20. Modes of 4 Segment Undamped String .....	57
Figure 21. Modes of 5 Segment Undamped String .....	59
Figure 22. Modes of 4 Segment Damped String .....	61
Figure 23. ARMA Model Coefficients of Damped String .....	64

## ACKNOWLEDGMENT

I wish to thank my thesis advisor, Professor Michael A. Morgan, for providing guidance and great assistance throughout this work.

This work is dedicated to my wife Orly and my sons Omer, and Roe, whom I love and appreciate very much as they endured this project.

## I. INTRODUCTION

### A. BACKGROUND

Investigations of transient scattered waveforms from conducting bodies have shown that it is possible to classify electromagnetic scatterers. Such research is particularly applicable to inverse scattering and radar target identification. Conceptual applications in radar target identification have been demonstrated in some laboratories using advanced, high resolution radar techniques. One type of technique is based upon the natural resonance modes which are part of the scattering response to an incident transient excitation. In 1971, Baum [Ref. 1], introduced the development of the singularity expansion method (SEM), which presents the response of a system as a weighted expansion of complex natural modes. Theoretical studies and experiments have shown that these modes are functions of the scatterer geometry and composition but are independent of the incident excitation, including aspect and polarization.

The fact that these natural modes are only functions of the target led to the idea to use them as a data base for the target identification process. This concept was introduced by Moffatt and Mains in 1974 [Ref. 2]. The identification process, in its most elementary form, includes a comparison against the modes that have been extracted and identified, using advanced signal processing techniques, as applied to the target's time-domain scattering response. Morgan showed that a complete

description of the scattered signal, using the conventional SEM approach, is valid only for the "late-time" portion of the scattered field [Ref 3]. This late-time scattering response is due to the source-free currents that remain after the incident field has completed its illumination of the target.

The unique properties of the late-time response are crucial to the development of algorithms to identify the resonance modes of the target. These natural resonance modes can be represented by pairs of conjugate poles in the left-half complex  $s$ -plane of the Laplace transform domain. Targets of different geometry, or composition, have different pole representations. Several techniques have been developed to extract the dominant poles in the time domain scattering responses of simple targets. Morgan [Ref 4], for example, introduced the classification of some kinds of electromagnetic scatterers by the annihilation of the natural modes. The advantages of this technique over others were achieved, primarily, by using only the late-time scattered field. The theory of natural resonance scattering is the basis for this thesis, and it is therefore explained in more detail in Chapter II.

## **B. PRESENTATION IN A DISCRETE MODEL**

Based on the theory of the natural resonance scattering one can recognize the late-time portion of the scattered signal as the response of a linear time-invariant (LTI) system. These kinds of systems can be numerically modeled and described by means of linear constant-coefficient difference equations [Ref. 5]. A discrete model, which describes the source-free current distribution, may explicitly present the late-

time response of the scatterer to an incident field as a function of its natural modes. Moreover, the currents may be described by an auto-regressive moving-average (ARMA) type model, having constant coefficients for the recursive terms which generate the natural resonance modes. This type of model represents an important class of discrete systems which are known as *recursive* systems since the output depends on previous values of the output. Such a discrete model can be employed in the process of identifying the resonance modes for electromagnetic and acoustic scatterers of various shapes. The time-independent coefficients of the recursive terms in the ARMA model are also the denominator polynomial coefficients of the system transfer function. Using the well-known concept of zeros and poles which represent the system frequency response, the roots of this polynomial are the poles which represent the complex natural frequencies of the resonance modes [Ref. 6]. In addition, such a discrete model gives a complete description of the natural resonance modes for a given scattering object when limited by the sampling frequency imposed by the Nyquist theorem. This is the basic idea of this thesis, in which such a model is set up for the case of the numerical finite-difference solution of the space-time wave equation. It is believed that this is the first time that such an approach has been presented.

### C. THESIS GOAL

The goal of this thesis was to investigate the possibilities of describing the natural resonance modes of electromagnetic and acoustic scatterers by discrete

ARMA models. These ARMA models should have constant coefficients for the recursive terms which determine the natural resonance modes. A model for a one-dimensional structure, such as the damped string with forcing function, illustrates the validity of the proposed approach. In addition, three-dimensional scattering structures can be analyzed using a space-time finite-difference method, which is an extension to the considered herein.

In this thesis an attempt have been made to present an overview of *some approaches* for solving the problem of the natural modes, and constructing the required model. A brief presentation of the theory of natural resonance modes, as developed through the time-domain integral equation, is included in Chapter II. Chapter III describes the simplified numerical solution, via the vector potential, as chosen to demonstrate the possibility of using an ARMA model for the case of an electromagnetic thin-wire. This technique is applied to the analogous problem of a finite string. Chapter IV presents the ARMA model with several analytical and computed results. Conclusions and a description of some future questions are discussed in Chapter V.

## II. THE THEORY OF NATURAL RESONANCE SCATTERING

### A. INTRODUCTION

The general topic to be considered in this chapter is the natural resonance mode representation for the induced current and the scattered field transient response of a perfectly conducting body. The case of a thin-wire is presented in some detail. The goal of this chapter is to provide the theoretical background required for constructing a discrete ARMA model for the natural resonances in electromagnetic scattering. In addition, the features of such a model should agree with this theory. A description of time-domain solutions relevant to this work are included in this chapter. There are two main steps in the process of setting up the ARMA model. First, the time-domain numerical solution is required, and second, based on the numerical solution, the discrete model must be constructed.

There are two independent techniques available for solving the problem of transient scattering. The first involves the computation of the frequency-domain response of the structure, followed by inverse Fourier transformation to yield the time-domain response. An alternative approach involves the direct formulation of either partial differential or integral equations in the time domain. One way of describing the scattered signal in terms of natural modes is by using the formalism known as the Singularity Expansion Method (SEM) [Ref. 1]. Mittra and Van Blaricum showed that the SEM pole singularities of a structure can be estimated

directly from its time-domain response [Ref. 7]. In this chapter time-domain integral equations are used general to represent solution of the transient electromagnetic problem. Also considered will be the conceptual basis of mode representations for fields and currents in transient scattering.

## B. TIME DOMAIN INTEGRAL EQUATIONS

Consider the general three-dimensional transient electromagnetic scattering problem as depicted by Fig. 1.

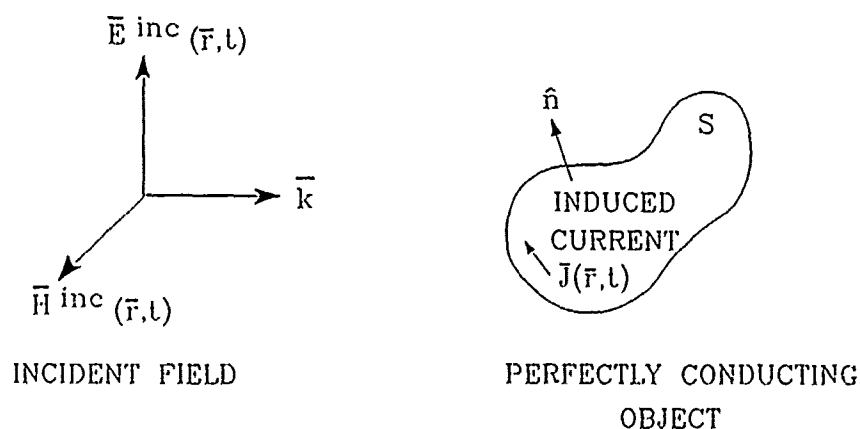


Figure 1. Transient Electromagnetic Scattering [After Ref. 4]

The perfectly conducting object is illuminated by an incident impulsive type plane wave in free space. The incident electric and magnetic fields are  $\vec{E}^{inc}$  and  $\vec{H}^{inc}$ ,



respectively. The integral equation approach represents the induced current on the surface of the object in terms of the incident field. There are two fundamental types of time-domain integral equations: the Electric Field Integral Equation (EFIE), and the Magnetic Field Integral Equation (MFIE). Derivations of both EFIE and MFIE are described by Mittra in detail [Ref. 8].

Integral equation derivations begin with the time-dependent forms of Maxwell's equations in free space. The continuity equation is used to relate the current density,  $\mathbf{J}_s$ , and the charge density  $\sigma$ . The scalar potential,  $\phi$ , and the vector potential,  $\mathbf{A}$ , are defined in terms of the electric and magnetic fields, respectively. The potentials are related to each other via the Lorentz condition [Ref. 8]. The wave equation can be derived independently for the scalar potential and for the vector potential using Maxwell's equations. The sources of the nonhomogeneous wave equations for the vector and the scalar potentials are the current density,  $\mathbf{J}_s$ , and the charge density,  $\sigma$ , respectively. The solution is constructed using the Green's function, which is the impulse response in time and space. The integral representation of the time-dependent electric and magnetic fields are obtained by applying the solutions of the potentials for the general current and charge distribution.

The expressions of the EFIE and MFIE, for the scattering problem are finally derived by applying the appropriate boundary conditions of the tangential electric and magnetic fields on the surface of the perfect conductor. In the case of the EFIE the sum of the tangential scattered electric field and the incident electric field is zero. The boundary condition in the case of the MFIE is that the total tangential magnetic

field is equal to the surface current density. The following equations are obtained for the EFIE (1) and MFIE (2), [Ref. 8]

$$\hat{n} \times E^{inc}(r, t) = \frac{\hat{n}}{2\pi} \times \int_S \left[ \frac{\mu_0}{R} \frac{\partial}{\partial \tau} J_s(r', \tau) - \frac{\sigma(r', \tau)}{\epsilon_0} \frac{R}{R^3} - \frac{1}{\epsilon_0} \frac{\partial}{\partial \tau} \sigma(r', \tau) \cdot \frac{R}{cR^2} \right] ds' \quad (1)$$

$$J_s(r, t) = 2\hat{n} \times H^{inc} + \frac{1}{2\pi} \hat{n} \times \int_S \left\{ \frac{1}{c} \frac{\partial}{\partial \tau} J_s(r', \tau) + \frac{J_s(r', \tau)}{R} \right\} \times \frac{R}{R^2} ds', \quad (2)$$

where  $S$  is the surface of the conductor, the unit vector which is outward normal to  $S$  is  $\hat{n}$ , the current density is  $J_s$ , the charge density is  $\sigma$ , the permeability and permittivity of free space are  $\mu_0$  and  $\epsilon_0$ , respectively. Further, the position vector is  $r$ ,  $r' \in S$  indicates points on the PEC surface,  $c = 1/(\epsilon_0 \mu_0)^{1/2}$  is the velocity of light,  $\tau = t - R/c$  is the retarded time, and  $R = |R| = |r - r'|$ .

Both the EFIE and MFIE are Principal Value (P.V.) integrals because of kernel singularities for  $r \rightarrow r'$ . The special forms of the time-domain integral equations (1) and (2) play fundamental roles in their solution construction. The main difference between these equations and their respective frequency domain equations is in the solution construction. The equations in frequency domain are handled numerically

by matrix inversion, while initial-value techniques are applied to time domain integral equations.

The solution of the general integral equation for the scattering problem uses a time-stepping technique. Special cases such as one- and two-dimensional scatterers, i.e, cylindrical and wire-type scatterers, have special forms of integral equations, hence construction of their solutions differ, considering numerical aspects and accuracy. For three-dimensional scatterers the MFIE is most convenient, while the EFIE is used in the case of thin wires and thin surfaces. This is due to the fact that for solid surface structures the kernel in the MFIE is less singular than the kernel in the EFIE. As a consequence, less sophisticated expansion functions may be employed for representing the unknown current. On the other hand, the MFIE becomes unstable for thin structures. The vector cross product between  $\mathbf{J}$  and  $\mathbf{R}$  in the Green's function may lead to computational difficulties by virtue of the small angle subtended, as in the case of the thin-wire [Ref. 9]. There is one unique feature of these integral equations for the induced surface current,  $\mathbf{J}_s$ , which is important to the discussion of natural resonance scattering. The unknown surface current,  $\mathbf{J}_s$ , inside the integral in both the MFIE and EFIE has the retarded time  $\tau$  argument. The retarded time  $\tau=t-R/c$  is always less than  $t$  since the P.V. integral excludes the point  $R=0$ . Considering this feature, the unknown current  $\mathbf{J}_s(t)$ , at any given time  $t$ , can be calculated from the MFIE in (2) using the known incident field at time  $t$  combined with the integral of terms which are known from the past history of the current. From another point of view, the effect of the source current at any point  $\mathbf{r}'$

is delayed by a time  $R/c$  in affecting the current at the observation point  $r$ . This point forms the basis of an iterative technique, termed *time-stepping*, for constructing the solution. The surface current may be determined by "stepping on" in time, thus eliminating the matrix inversion required for the numerical solution of the frequency domain integral equation. Figure 2 shows the region of interaction in space-time for the one-dimensional case  $(x,t)$ . This region is defined by  $ct - |x - x'| < 0$  and denoted by the shaded area.

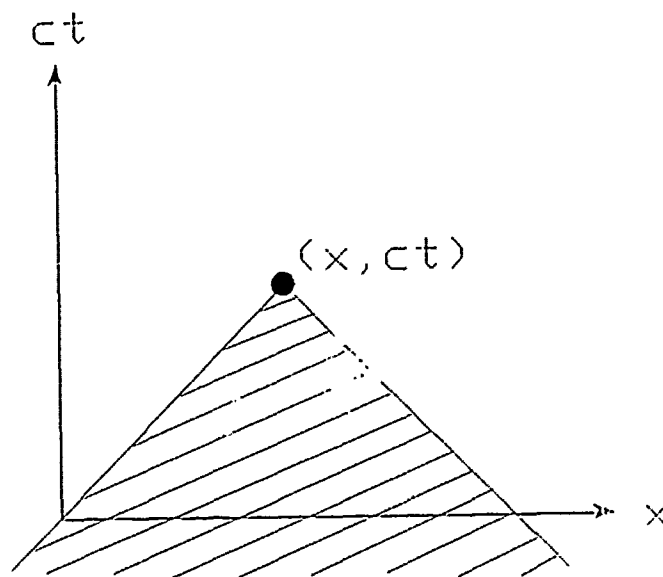


**Figure 2. Region of Interaction**

The same general procedure can be similarly employed for solving the EFIE

(1). The current at the spatial point of observation, and at some time  $t$ , can be

calculated in terms of the known incident electric field at that same spatial point and time, and from the integral of terms involving retarded time [Ref. 8]. This point is further illustrated in the case of a thin-wire.

### C. NATURAL RESONANCE SCATTERING

The following discussion is based upon the theory described by Morgan [Ref. 4]. The MFIE (2) describes the induced current on the surface of the object in terms of the incident field or "physical optics" part, and in terms of the "feedback" current. Figure 3 shows the situation in transient scattering. An incident field with short pulse duration illuminates the scatterer. In the case of a radar it can usually be considered a plane wave. Once illumination of the object is completed, for  $t > t_L$ ,  $\mathbf{H}^{inc} = 0$ , and only the source-free currents remain on the object, generating the natural modes. These modes are of the form  $\mathbf{J}_n(\mathbf{r}) \exp(s_n t)$ , where the natural resonance frequencies  $s_n = \sigma_n + j\omega_n$  are functions of the scatterer geometry and composition. The SEM representation of the current takes the form of a summation of damped sinusoids which can be expressed using complex exponentials as

$$\mathbf{J}(\mathbf{r}', t) = \sum_{m=-\infty}^{\infty} A_m \mathbf{J}_m(\mathbf{r}') e^{s_m t}, \quad t > t_L. \quad (3)$$

Since  $\mathbf{J}(\mathbf{r}', t)$  is real, the complex exponents  $s_m$ , which are poles in the complex frequency plane, and the weight coefficients  $A_m$  come in conjugate pairs. For a practical incident field, having a finite bandwidth, only a limited number (say  $N$ ) of

natural resonance modes will be "significantly" excited. The scattered field which is generated by the induced current is composed of two parts; an early-time driven response and a late-time natural mode response [Ref 4]. The early-time scattered field can be described as a linear combination of two terms. The first is an aspect-dependent physical optics term.

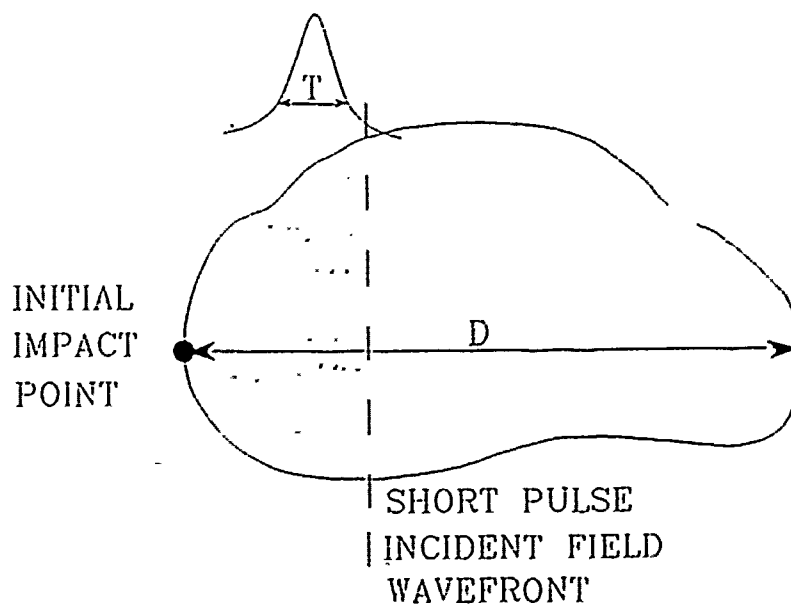


Figure 3. Short Pulse Wave Illumination [After Ref. 4]

The second term describes the scattered field due to the source-free current distribution. These currents are integrated over the time-varying portion of the surface to get the contribution from all previously illuminated points which are dot-shaded in Fig. 3. This term can be represented by the SEM expansion having the

same exponential resonance terms with time-varying coefficients (SEM class 2). The late-time scattered field is due to the source-free currents that remain after the incident field has completed its illumination of the scatterer. The late-time starts after a delay of  $T_0 = T + 2D/c$  from the initial impact of the incident field on the object, where  $T$  is the practical incident field pulse width, and  $D$  is the length of the object in the direction normal to the wavefront of the incident field. At time  $T_0$  the integral is calculated over a fixed surface area, and thus the SEM representation for the late-time is a summation of the same exponential resonance terms with constant coefficients (SEM class 1).

In summary, the monostatic transient scattered signal waveform can be described in the following form [Ref. 4]

$$y(t) = y_E(t) \cdot [U(t) - U(t - T_0)] + y_L(t) U(t - T_0) + N(t) \quad (4)$$

where  $U(t)$  is the Heaviside unit step function,  $y_E(t)$  is the early-time response,  $y_L(t)$  is the late-time response, and  $N(t)$  describes the measured noise and other signal pollutants. The late-time portion of the scatterer response to such an incident field, with its unique features, is considered in the process of this research. The discrete form of the late-time response is obtained in order to set up the required ARMA model.

#### D. THIN WIRE CASE

Consider the case of a perfectly conducting cylindrical thin-wire scatterer. The geometry of the problem is shown in Fig. 4. The radius of the wire,  $a$ , is small compared to the wire length,  $L$ . The radius,  $a$ , is also small compared to the shortest significant incident field wavelength,  $\lambda$ .

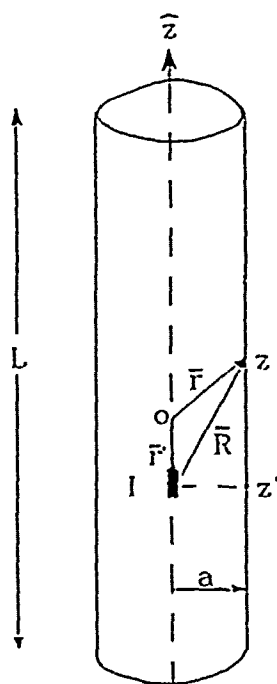


Figure 4. Geometry of a Cylindrical Thin Wire Scatterer

In this case the thin-wire approximation is applicable; that is, the azimuthal surface current is negligible compared to the axially-directed component. Then the surface



current density,  $J_s$ , can be written as

$$J_s(z) = \frac{I(z)}{2\pi a} \hat{z} \quad (5)$$

where  $\hat{z}$  is a tangential unit vector pointing in the axial direction. The current is a function of  $z$  only. The incident electric field  $E^{inc}$  has contribution to the surface current only in the  $\hat{z}$  direction. Under these conditions the integral equation for this case can be written, using the EFIE type (1), as

$$\begin{aligned} 4\pi E_z^{inc}(z, \tau) = & \int_0^L \frac{\mu_0}{R} \frac{\partial}{\partial \tau} I_z(z', \tau) dz' \\ & + \frac{1}{\epsilon_0} \int_0^L \frac{(z-z')}{R^3} \int_{-\infty}^{\tau} \frac{\partial}{\partial z'} I_z(z', \tau') d\tau' dz' \\ & + \frac{1}{\epsilon_0 c} \int_0^L \frac{(z-z')}{R^2} \frac{\partial}{\partial z'} I_z(z', \tau) dz' \end{aligned} \quad (6)$$

where  $R = r - r'$  is the vector from the current element along the  $z$  axis pointing to the point of observation on the surface of the wire,  $|R| = [(z-z')^2 + a^2]^{1/2}$ , while  $\tau = t - R/c$  is the retarded time. The integral in (6) is not a P.V. type integral since  $r' \neq r$ .

There are several approaches to solve the thin-wire integral equation arising in time-domain scattering problems. The interpolation procedure and the finite-difference approach are presented in [Ref. 8]. The general interpolation procedure is to subsectionalize the thin-wire by dividing it into  $N$  segments and then to define a set of basis functions for expressing the unknown current,  $I$ , in each of these segments. Similar segmentation is also necessary for the time domain, choosing the appropriate time interval with regard of the spatial interval. An interpolation scheme in time and space is then used to express the current at one node (space and time) in terms of the current values in the neighboring nodes. The final step is to describe the thin-wire integral equation using the expansions and apply point matching to generate the desired matrix equation.

A second approach is to use the finite-difference method to approximate the differential operators appearing in the time-domain integro-differential equation. This approach was introduced by Sayre and Harrington [Ref. 10] where the EFIE is written in terms of the vector potential  $A$ . The solution for the vector potential  $A$  can be based on the finite-difference method, as applied to the driven wave equation. In fact, aside from the specified boundary conditions, the solution has the same form as will be employed in the acoustic string case in the following chapter.

## **E. SUMMARY**

The late-time portion of the scatterer response can be represented by a weighted summation of natural modes. The modes are functions of the scatterer

geometry and *not* of the incident excitation. The EFIE which describes the surface current on the scatterer can be solved numerically for the case of a thin-wire.

Although, in principle, the ARMA representation can be derived by discretizing an integral equation, the full topological connectivity wrought by the Green's function yields an imposing difficulty. A better approach is found by employing the finite-difference approach, with its "nearest-neighbor" connectivity. This will be presented in Chapter III.

### III. ELECTROMAGNETIC AND ACOUSTIC SCATTERING EXAMPLES

#### A. INTRODUCTION

Open region electromagnetic and acoustic scattering and radiation problems can be formulated using the integral equation approach. Other techniques may also be applied to these problems, both in the frequency- and time-domains. One of these methods is the finite-difference scheme which provides a convenient means for deriving a time-stepping algorithm for solving the EFIE. In this work, an exclusive use of this method has been utilized to formulate the problem of transient scattering via the time-space wave equation, and to demonstrate the new approach of presenting the late-time scattering response in a discrete ARMA model.

The objective of this chapter is to describe the numerical solution chosen for this research. The derivation of the EFIE expressed in terms of the vector potential is presented. An analogous case of a vibrating string of fixed length is then described in conjunction with various methods of solution to complete the theory of the analog form of the problem. A discrete form of the time-space wave equation using the finite-difference method is then presented along with pertinent numerical considerations.

The wave equation with forcing term describes numerous physical phenomena such as a driven finite string or an illuminated transmission line. A computer program entitled TH7.FOR was written to support this research, and a source listing is given

in Appendix A. The program provides the solution of the inhomogeneous time-space wave equation. The string (or transmission line) can be excited by a Gaussian pulse from different angles of incidence. The amplitude and width of the Gaussian pulse excitation, as well as the number of segments on the string can be independently selected by the user. Results in time-space are presented for different cases. Fast Fourier transforms (FFT) are used to obtain the frequency-domain results from the time-domain data. Results in these cases are also presented showing agreement with the basis of the natural resonance scattering theory. Time-domain data provided by the computer program was also used to check the ARMA model and is presented in Chapter IV.

## B. DERIVATION OF THE VECTOR POTENTIAL EQUATION

The Electric Field Integral Equation (EFIE) may be written in terms of the vector potential  $A$ . The derivation begins with a slightly different form of the EFIE. The scattered electric field, produced by the induced current, may be written in terms of the scalar potential  $\phi$ , and the vector potential  $A$ , as

$$E(r,t) = -\frac{\partial A}{\partial t} - \nabla\phi . \quad (7)$$

The scalar potential  $\phi$  can be expressed in terms of  $A$ , via the Lorentz condition, as

$$\nabla \cdot A(r,t) + \mu_0 \epsilon_0 \frac{\partial}{\partial t} \phi(r,t) = 0 . \quad (8)$$

Applying the boundary condition of the electric field on the surface of a perfectly conducting body in order to write Eq. (7) in terms of the scattered field, and using the Lorentz condition to write Eq. (7) in terms of the vector potential, the tangential component of Eq. (7) can be written as

$$\hat{n} \times E^{inc} = \hat{n} \times \frac{\partial A}{\partial t} - \frac{1}{c^2} \int_{-\infty}^t \hat{n} \times \nabla \nabla \cdot A dt', \quad r \in S. \quad (9)$$

Equation (9) is differentiated with respect to time to eliminate the integral. This yields the following equation

$$\hat{n} \times \frac{\partial E^{inc}}{\partial t} = \hat{n} \times \frac{\partial^2 A}{\partial t^2} - \frac{1}{c^2} \hat{n} \times \nabla \nabla \cdot A, \quad r \in S, \quad (10)$$

where the expression for the vector potential  $A$  in terms of the induced surface current  $J_s$  is

$$A(r, t) = \frac{\mu_0}{4\pi} \int_S \frac{J_s(r', t - R/c)}{R} ds'. \quad (11)$$

Equation (10) may be reduced to the one-dimensional case of the cylindrical thin wire along the  $x$ -direction, with length  $L$  and radius  $a$ , under the assumptions described in Chapter II. The following equation is obtained

$$\frac{\partial^2 A}{\partial x^2} - \frac{1}{c^2} \frac{\partial^2 A}{\partial t^2} = -4\pi \epsilon_0 \frac{\partial E^{inc}}{\partial t}. \quad (12)$$

The vector potential in Eq. (12) is defined in a slightly different manner from Eq. (11). The vector potential  $A$  is defined as

$$A(x,t) = \int_0^L \frac{J_z(x', t-R/c)}{R} ds', \quad (13)$$

with  $R = [(x-x')^2 + a^2]^{1/2}$ .

For the purpose of this work it was found convenient to modify equation (12). The term which includes the incident field is replaced by the function  $f(x,t)$  which describes the pulse excitation. A term which describes loss was added in order to investigate cases where damping was included as well. The final equation, which has been solved numerically by computer program, has the following form:

$$\frac{\partial^2 U(x,t)}{\partial x^2} - \frac{1}{c^2} \frac{\partial^2 U(x,t)}{\partial t^2} - \xi \frac{\partial U(x,t)}{\partial t} = f(x,t), \quad (14)$$

where the function  $U(x,t)$  satisfies the expression, and  $\xi$  is the positive coefficient of the loss term. When  $\xi=0$  the equation is reduced to the lossless case which is simply the nonhomogeneous wave equation. The last step is to define the boundary and the initial conditions in order to completely describe this problem. Homogeneous boundary conditions have been set in this case to present a total reflection at the ends of a string. This formulation also represents the cases of short or open circuits at the ends of an excited TEM mode transmission line. In the

electromagnetic case the potential on the ends of the single wire scatterer is non-zero and is thus not properly represented by the wave equation solution considered here.

In terms of the function  $U(x,t)$  the boundary conditions may be written as  $U(0,t)=U(L,t)=0$ . The initial conditions can describe the voltage or current on the transmission line before the incident field impacts. There is assumed to be no initial voltage or current. Likewise, the string is initially at rest in the acoustic case. These conditions are formulated by homogeneous initial conditions as  $U(x,0)=0$ , and  $\partial U(x,0)/\partial t=0$ , where  $0 \leq x \leq L$ . Note that homogeneous initial conditions may be replaced by some functions  $U(x,0)=h(x)$  and  $\partial U(x,0)/\partial t=g(x)$ , where  $0 \leq x \leq L$ , in order to make the partial differential equation (PDE) homogeneous. This point is further illustrated by the ARMA model presentation.

### C. VIBRATING STRING WITH FORCING FUNCTION

The case of a thin wire is analogous to the problem of a vibrating string of fixed length. This problem is thoroughly discussed in the literature, including [Ref. 10] which covers this topic in considerable detail. The formulation of a vibrating string problem is

$$\frac{\partial^2 U(x,t)}{\partial x^2} - \frac{1}{c^2} \frac{\partial^2 U(x,t)}{\partial t^2} = 0, \quad (15)$$

with the boundary conditions  $U(0,t)=0$ ,  $U(L,t)=0$ , and initial conditions  $U(x,0)=h(x)$ , and  $\partial U(x,0)/\partial t=g(x)$ . Several methods are available to solve the problem of a



vibrating string of fixed length. One way to solve it is by separation of variables. This yields the eigenvalues and eigenfunctions corresponding to the homogeneous boundary conditions. A Fourier series method is then used to satisfy the initial conditions. This is found to be a convenient means to solve the problem in many cases. However, difficulties may arise due to the complexity of some initial condition functions which must be integrated. One applicable example in the case of transient scattering could be the function which describes a Gaussian pulse excitation.

An equivalent technique, but in some ways more useful, is the "method of characteristics". In this approach the d'Alembert's solution is applicable [Ref. 11], with the following form

$$U(x,t) = \frac{h(x-ct) + h(x+ct)}{2} + \frac{1}{2c} \int_{x-ct}^{x+ct} g(x') dx'. \quad (16)$$

The solution is valid for the region defined by  $0 < x-ct < L$  and  $0 < x+ct < L$ . This region is shown dot-shaded in Fig. 5 which describes points of position and time such that signals from the boundary have not already arrived. The modification to the solution is made considering the boundary conditions which, in turn, imply multiple reflections as illustrated in Fig. 6. The simplest way to obtain the solution is to extend the initial condition functions as odd functions (around  $x=0$ ) with period  $2L$ . With these odd periodic initial conditions, the method of characteristics can be utilized as well as d'Alembert's solution (16).

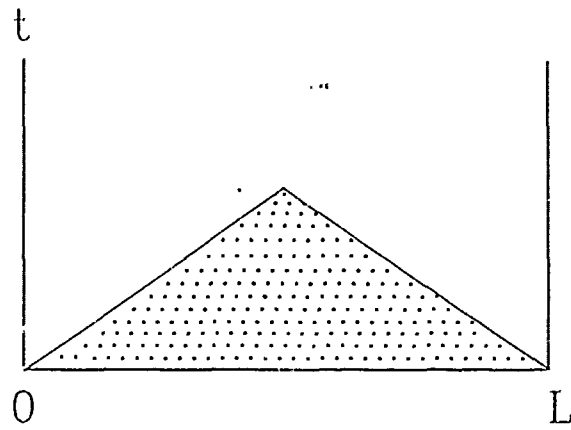


Figure 5. Characteristics [From Ref. 11]

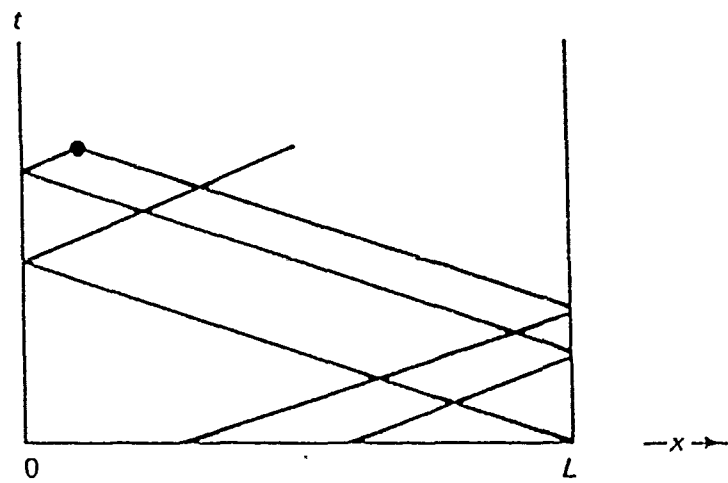


Figure 6. Multiple Reflected Characteristics [From Ref. 11]

#### D. FINITE-DIFFERENCE APPROXIMATION TO THE WAVE EQUATION

The discrete form of Eq. (14) is required for the numerical solution. In general, numerical solutions are required in cases where the shape of the area of integration or changes to the boundary and initial conditions make analytical solutions impossible. These changes do not fundamentally affect finite-difference methods although sometimes modifications to the methods are necessary. In this work the finite-difference method was used to approximate the derivatives in Eq. (14), and to make use of the time-stepping algorithm previously mentioned.

The finite-difference method may be derived based on a Taylor's series approach. The idea is to approximate the function  $U(x)$  at a point near  $x=x_0$ , e.g.,  $(x_0 \pm \Delta x)$ , using the polynomial approximation of the Taylor series. Through the use of Taylor series, it is possible to approximate derivatives in various ways. A finite-difference approximation for a derivative can be written using forward difference, backward difference or central difference. The central difference is found to be more accurate [Ref. 11] and it was used in this work.

Using the central difference formula, the first partial derivative is written as

$$\frac{\partial U}{\partial x}(x_0, y_0) \sim \frac{U(x_0 + \Delta x, y_0) - U(x_0 - \Delta x, y_0)}{2\Delta x}, \quad (17)$$

and the second derivative as

$$\frac{\partial^2 U}{\partial x^2}(x_0, y_0) \sim \frac{U(x_0 + \Delta x, y_0) - 2U(x_0, y_0) + U(x_0 - \Delta x, y_0)}{\Delta x^2}. \quad (18)$$

Figure 7 shows the discrete space-time plane of the finite string problem. The string length  $L$  is subdivided into  $N$  segments with  $\Delta x = L/N$  being the spatial interval. The time interval is chosen to be  $\Delta t = \Delta x/c$ , where  $c$  is the velocity of propagation. The notation  $U_i^j$ , with the spatial segment  $i$  and the time segment  $j$ , is used to describe the function  $U(x,t)$ , where  $x = i\Delta x$  and  $t = j\Delta t$ .

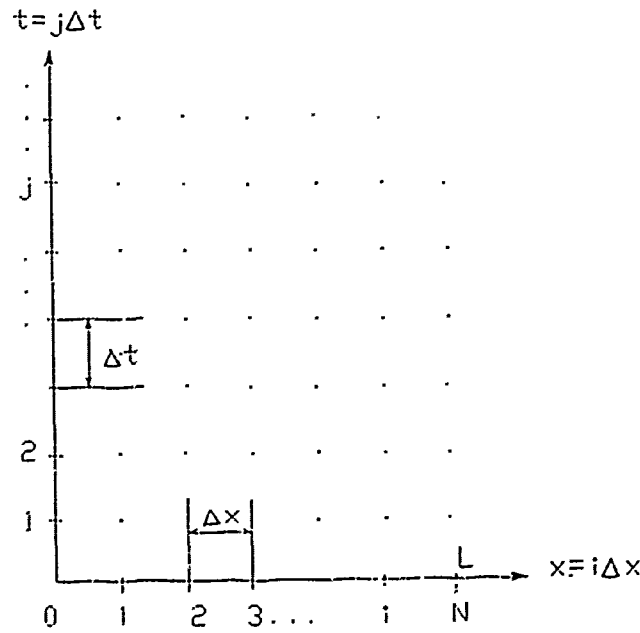


Figure 7. Space-Time Discretization

The approximated PDE for Eq. (14) may be written as

$$\frac{U_{i+1}^j - 2U_i^j + U_{i-1}^j}{\Delta x^2} - \frac{1}{c^2} \frac{U_i^{j+1} - 2U_i^j + U_i^{j-1}}{\Delta t^2} - \xi \frac{U_i^{j+1} - U_i^{j-1}}{2\Delta t} = f_i^j. \quad (19)$$

The relation between the space interval and the time interval may be used in Eq. (19) to yield Eq. (20). Equation (20) is written for  $U_i^{j+1}$  in a form called the *star operator*. The star operator is illustrated in Fig. 8.

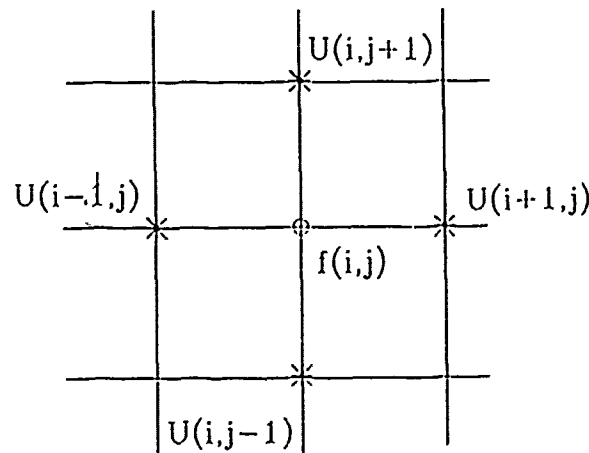


Figure 8. Star Operator

Equation (20) describes the standard five-point finite-difference approximation to the Laplacian  $\nabla^2$  with slightly different weights.

$$U_i^{j+1} = A[U_{i+1}^j + U_{i-1}^j] + P U_i^{j+1} + D f_i^j, \quad (20)$$

where

$$A = \frac{2}{2+cl}, \quad P = \frac{cl}{2+cl} - A, \quad D = -A \Delta x^2, \quad cl = c \xi \Delta x.$$

Note that when  $\xi = 0$ , which is the lossless case,  $cl = 0$ ,  $A = 1$ ,  $P = -1$ , and  $D = -\Delta x^2$ . The star operator is used to describe the finite-difference equation in a simple way. Note that in this case the value of  $U_i^j$  does not contribute since  $\Delta t = \Delta x/c$ . Given the initial

and boundary conditions, which are homogeneous in this case, the values of the function  $U_i^j$  at any point  $(i,j)$  can be calculated by marching forward in time using the star operator. This is the solution procedure applied in the computer program given in Appendix A.

## E. NUMERICAL CONSIDERATIONS

In any application of numerical solutions, the questions of accuracy, stability, and information bandwidth must be resolved. This section includes a discussion of some numerical aspects which are relevant in this case.

The finite-difference approximation to the first derivative is consistent, meaning that the truncation error vanishes as  $\Delta x \rightarrow 0$ . Hence, the exact solution is expected to converge as the number of segments increases. The sampling rates in the spatial and temporal domains are key factors in determining the accuracy of the numerical solution. The spatial sampling rate should be high enough to adequately resolve the spatial variation of the incident field as it propagates past the scatterer. The time sampling space should be high enough to adequately resolve the time variation of the pulse excitation. However, the sample points in time are not independent of the space interval. Correlation between them is required because of equivalence between space and time in the retardation effect. Since the interactions between the currents on different points on the scatterer depend upon the velocity of propagation, the time sample spacing,  $\Delta t$ , must be related to the space sample interval,  $\Delta x$  by  $c\Delta t \leq \Delta x$  [Ref. 9]. This is also known as the *Courant stability condition* for the wave equation [Ref

11]. The inequality is equivalent to requiring that the space sample points be at least as far apart as the distance the electromagnetic wave travels, with velocity  $c$ , in the interval between two sample points in time. The relation between  $\Delta t$  and  $\Delta x$  determine the stability of the solution. The idea is that the numerical process should limit the amplification of the initial conditions. In this simple case of a finite string, the time sample spacing is related to the space sample interval by  $c\Delta t = \Delta x$ .

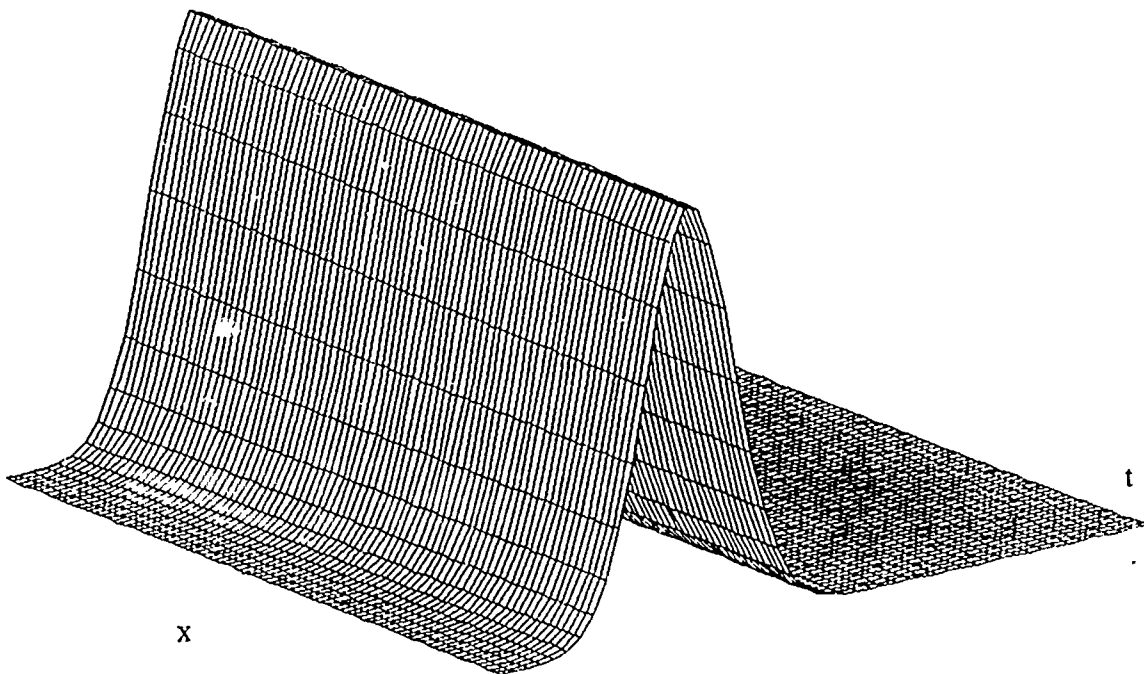
Among the factors which determine the sampling rate are the shape and the width of the incident field pulse, the scatterer size relative to the pulse width, and the highest frequency natural mode to be obtained by the solution. A delta function space-time impulse whose frequency spectrum extends from zero to infinity with uniform amplitude is desired. However, this is impossible from a practical standpoint. The approximation is made by a Gaussian impulse since it rapidly decays to zero. The same property is applicable in the frequency-domain, where the amplitude rapidly decreases with increasing frequency. In order to adequately resolve the incident field in time and space the appropriate sample spacing, which result in reasonably accurate numerical results, have been found to be on the order of one-fifth and up to one-tenth the pulse width in time and space, respectively. The pulse width is determined by the scatterer size and the highest frequency information required.

## F. COMPUTED RESULTS

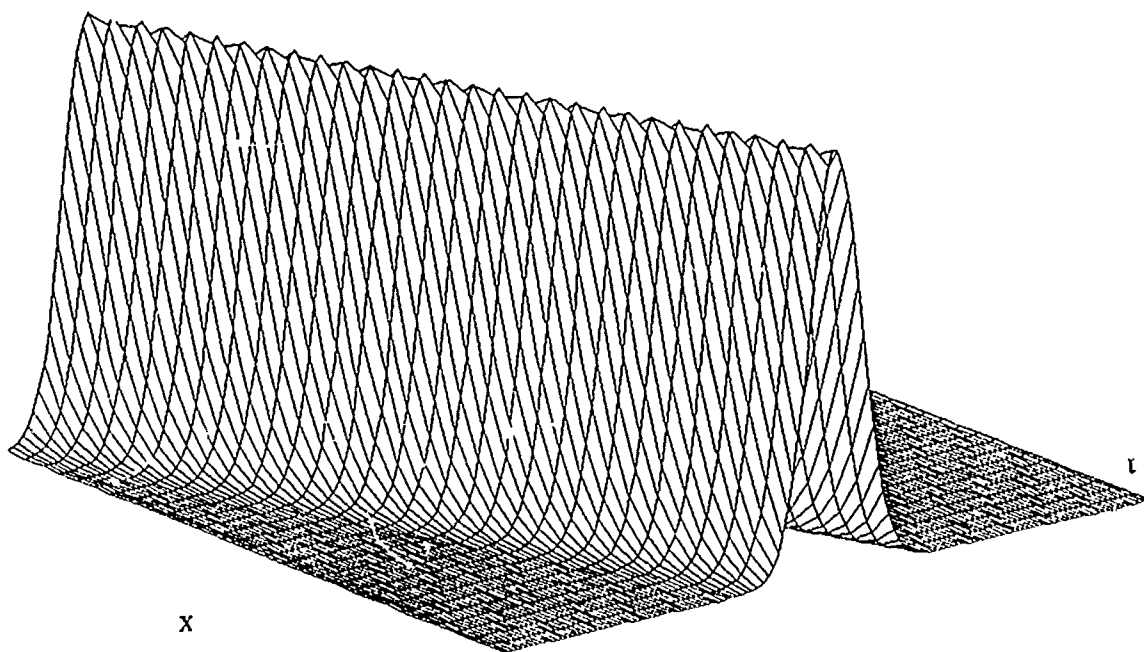
A computer program was written to obtain time-domain results to support this investigation. The program numerically solves Eq. (14) using the finite-difference method. The solution is determined using the procedure described in previous sections and the pulse shape is Gaussian. Gaussian pulse parameters such as pulse width, amplitude, and angle of incidence can be changed independently by the user to provide results for different cases. Additional parameters such as string length, number of segments on the string, time delay for peak pulse impact, and the number of time steps to be computed can also be varied. The coefficient  $\xi$ , for the case of loss, can be altered by the user within the program to investigate lossy cases. Note that for  $\xi=0$  the program will solve for the lossless case. Figure 9 shows the Gaussian pulse excitation for different angles of incidence. Broadside pulse excitation is shown in Fig. 9(a), and Fig. 9(b) shows the pulse excitation for a 60 degree incident angle. In both cases there are 10 time samples in the pulse width, where the pulse width is defined between the points at which the amplitude is 10% of the maximum.

Figures 10 and 11 show some results in the space-time domain. Figure 10 shows the displacement on the string along 200 time steps for the case of broadside excitation. A one-meter "electromagnetic string" was assumed, with  $c=3 \times 10^8$  m/s. The one-meter length was subdivided into 15 segments which results in a space interval of  $1/15$  meter. The time interval is related to the space interval by the velocity of light  $c$ , which gives  $\Delta t = (\Delta x/c) = 0.22$  ns. The pulse excitation has a Gaussian shape with pulse width of 2.0 ns. Figure 10a shows the result for the





(a) Broadside Excitation

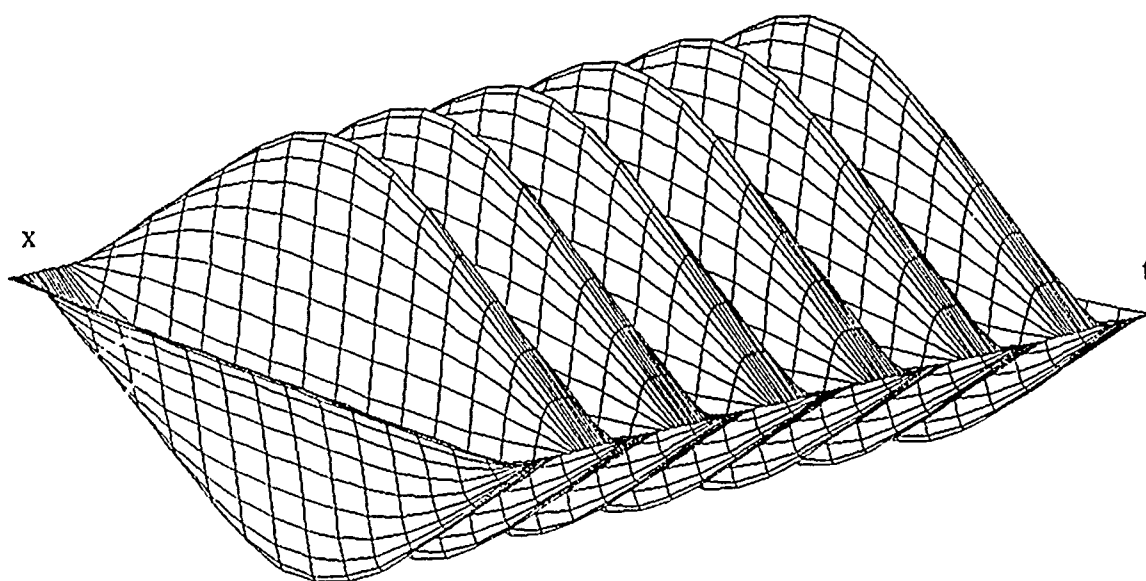


(b) 60 Degrees Excitation

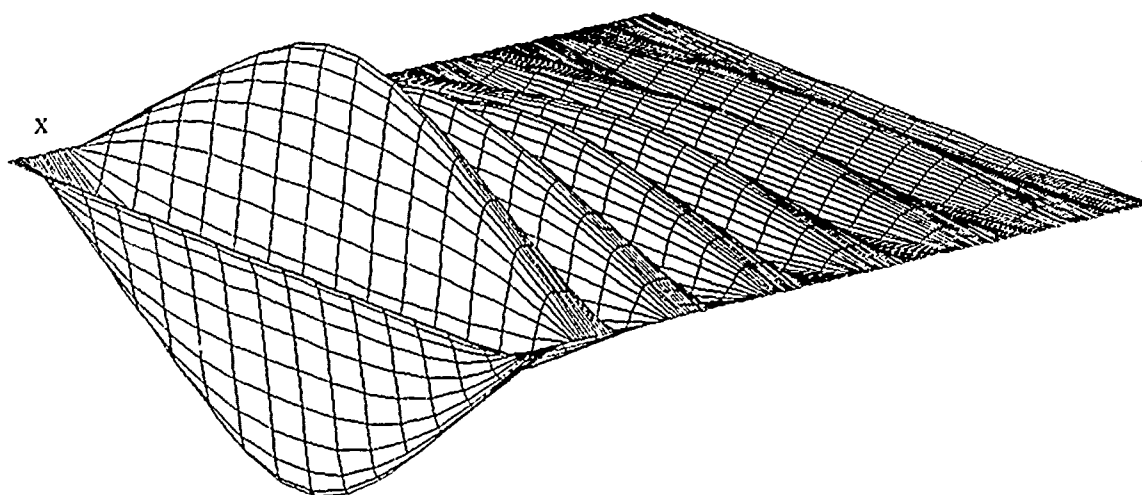
Figure 9. Gaussian Pulse Excitation

lossless case and Fig. 10b is the case with loss added to the system by setting the value of the coefficient  $\xi$  in equation (20) to be non-zero and positive. In these cases, when the string is excited by a broadside Gaussian pulse, the displacement is symmetric along the string. Symmetry is observed about the center of the string due to the symmetric boundary conditions, initial conditions and driver. The difference between the lossless case and the lossy case is in the amplitude. The displacement of each segment is a periodic function with a period of  $2N$  time steps where  $N$  is the number of segments on the string, except in the early-time when the incident pulse is still exciting the string. This point is illustrated in Fig. 11. In this figure, the displacement of segments number 2 and 8 are presented for the lossy case having periodic propagation except when the string is excited by the incident pulse. The period is 30 time steps which is exactly  $2N$  for  $N=15$  segments. The early-time is about 15 time steps including several time steps before the pulse starts.

Figures 12a and 12b show results for the case of 30 degree incident angle on the Gaussian pulse. All other parameters are the same as for the case illustrated in Fig. 10. As expected the displacement of the string is asymmetric. The early-time in this case is longer than in the case of broadside excitation since it takes more time for the incident pulse to complete its excitation of the string. The time-domain characteristics in these results did not change. Both have the same period ( $2N$  time steps). Figure 12a shows the results for the lossless case and Fig. 12b for the lossy case.



(a) Lossless Case



(b) Lossy Case

Figure 10. String Displacement for Broadside Excitation

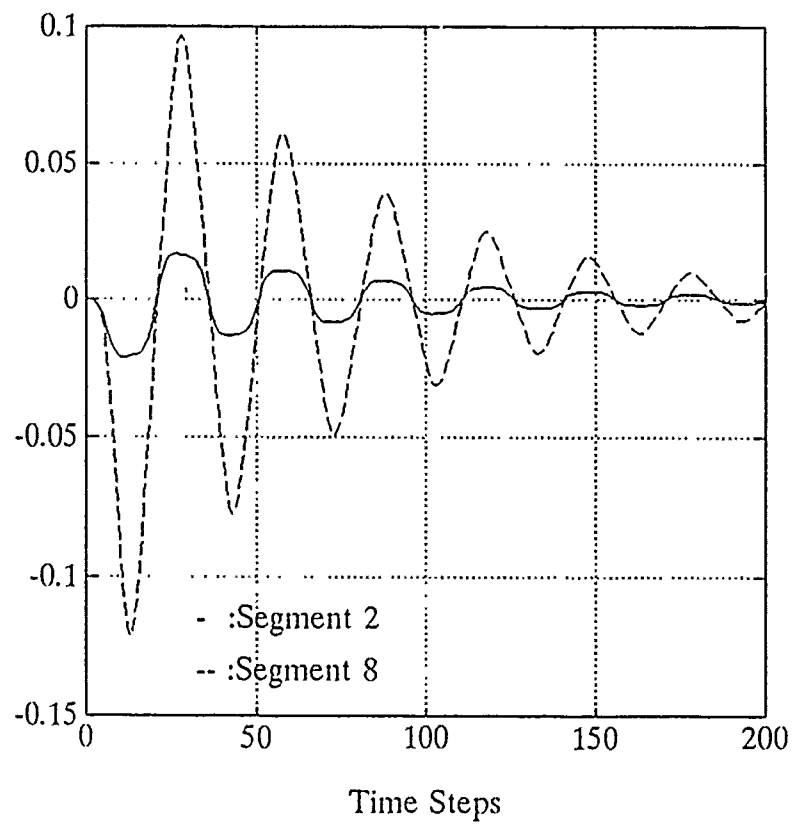
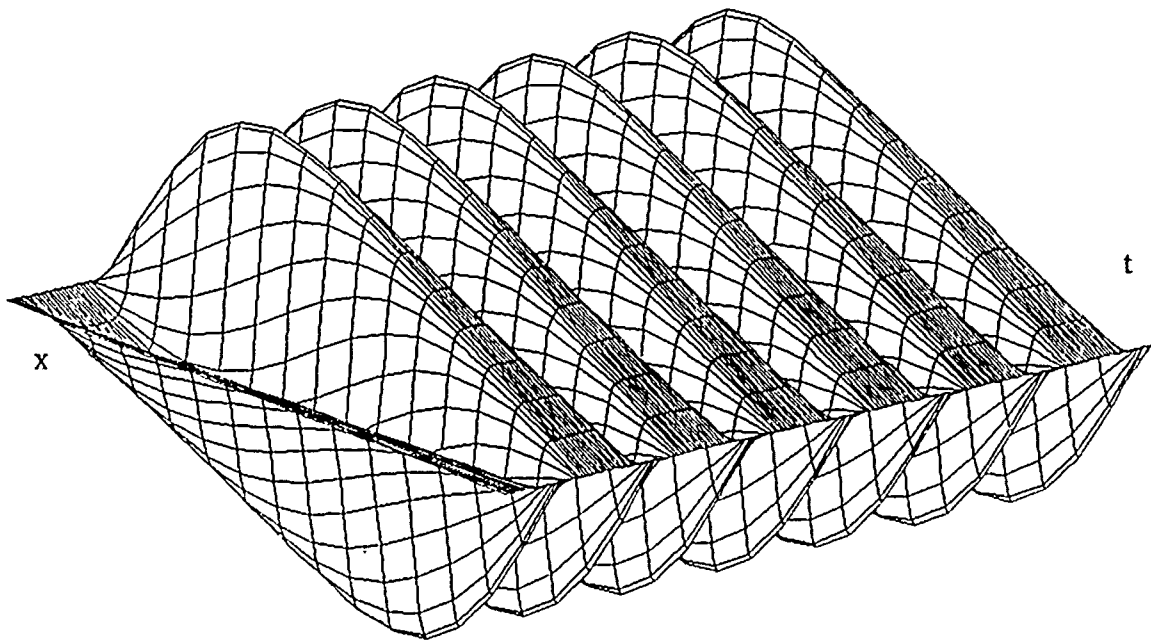
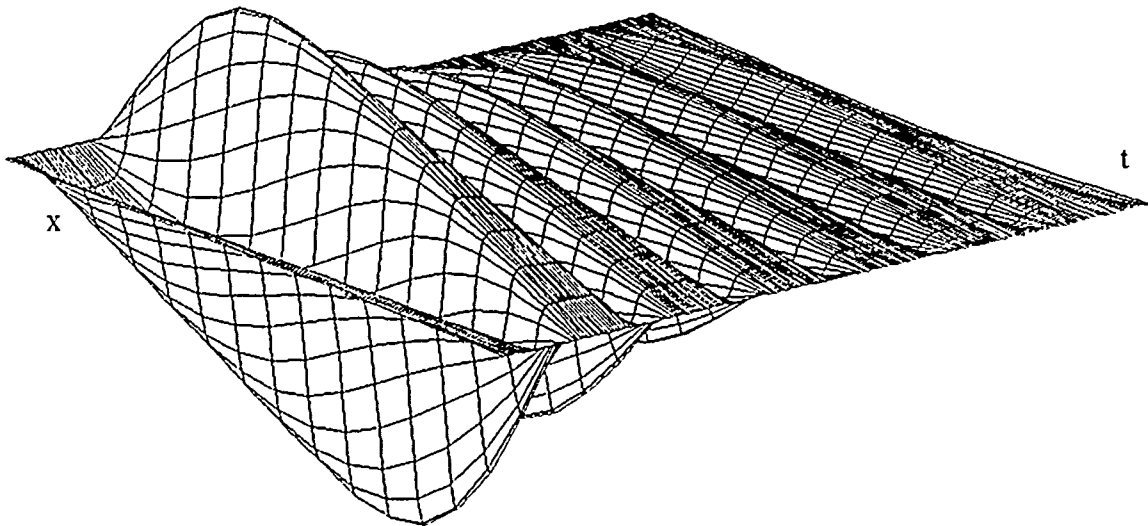


Figure 11. Displacement of Segments 2 and 8 (Lossy Case)



(a) Lossless Case



(b) Lossy Case

Figure 12. String Displacement for 30 Degree Incident Angle

Time-domain results were further processed to obtain frequency-domain results using the Fast Fourier transform (FFT). The objective was to check the time-domain results against the natural resonance mode theory. The frequency spectrum of the displacement on each segment was checked in order to analyze the resonance mode presentation as a function of the position on the string. The procedure includes computation of the spectrum of the displacement as a function of time for each segment on the string using the FFT. A representative example is shown in Figures 13 and 14, where time-domain data of Fig. 12 was used in this case. There are 15 segments on the string and the incident angle is 30 degrees. Figure 13 shows the frequency spectrum of the displacement of segments number 3, 6, and 11. It is clear that the modes have the same frequencies for these segments, although each with different energy depending on position. Figure 14 shows similar results to that of Fig. 13, but for all the segments on the string. At this point a tentative conclusion may be made that the resonance mode frequencies are independent of the position on the string. Note that the FFT of 256 points was taken using the data including the short early-time data. In this case, the early-time data may be used since this portion also includes information about the modes. Figure 15 shows the frequency spectrum in the case of broadside excitation and with the same parameters as in the case of 30 degree incident angle (Fig. 13). The differences between the results are explicitly presented. In the case of broadside excitation, only even modes are excited while in the case of the 30 degree incident angle both even and odd modes are excited.

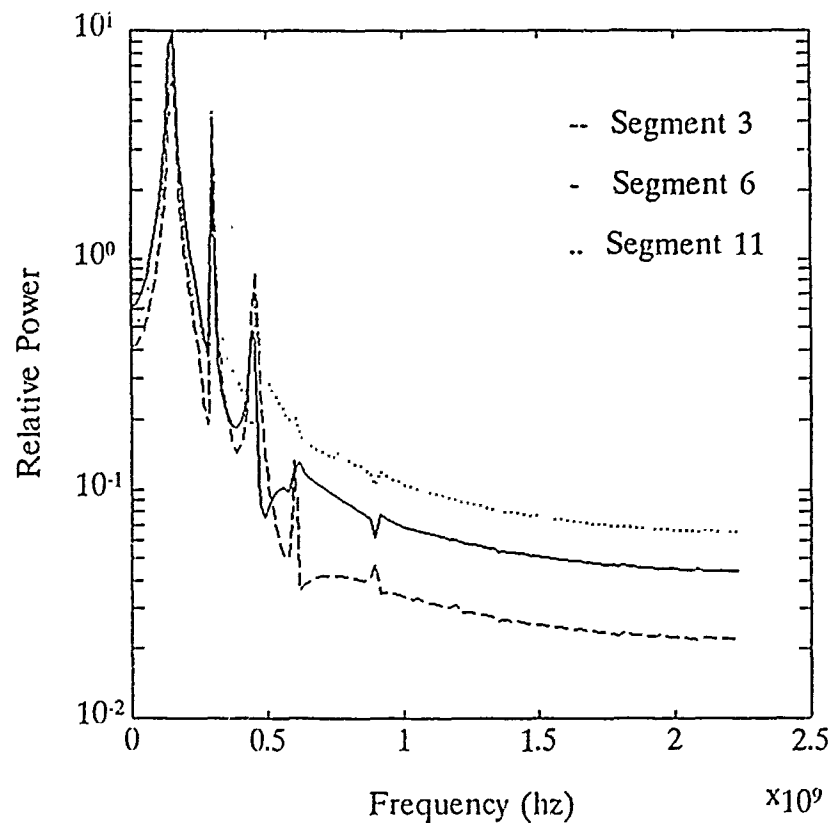


Figure 13. Resonant Frequencies (30 Degrees)

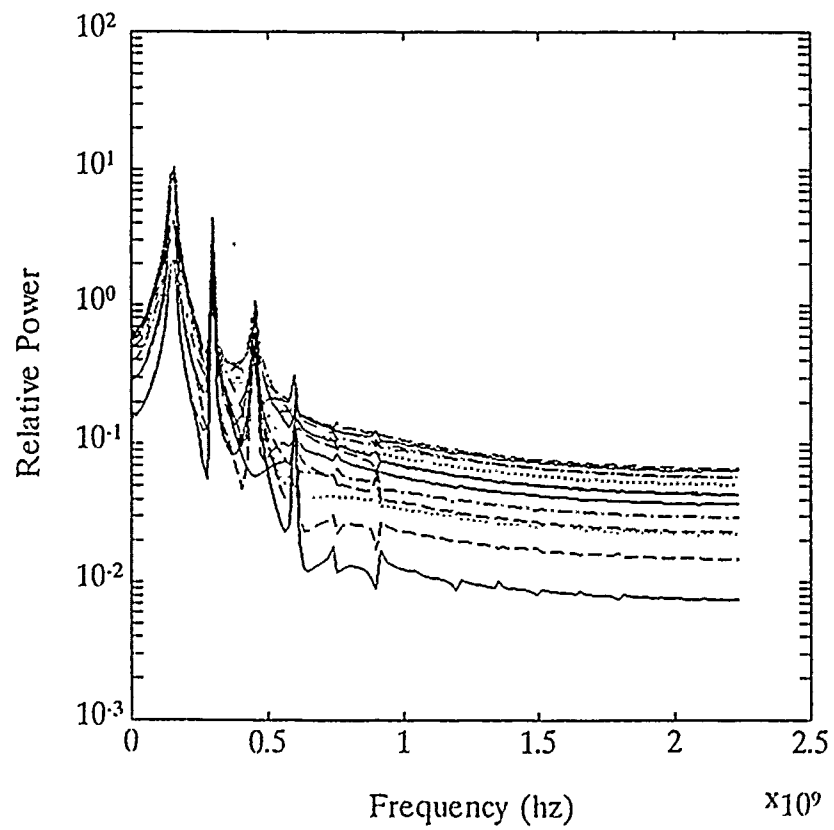


Figure 14. Modes of All Segments (30 Degrees)



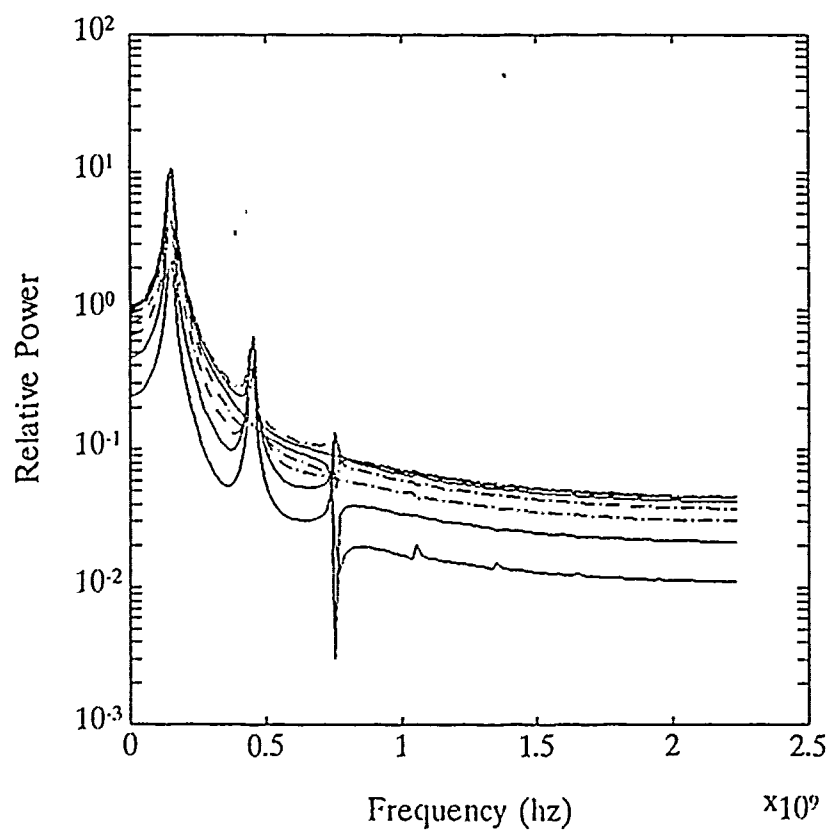


Figure 15. Modes of All Segments (Broadside)

The fact that these modes are aspect-independent may be checked in the frequency-domain by using the time-domain data for different incident angles. Figures 16 and 17 show results for various incident angles. The string was subdivided into  $N=25$  segments. The Gaussian pulse width was set to 2 nanoseconds in order to allow 15 samples in the 10% pulse width. These parameters result in a sampling frequency to be 7.5 Ghz, thus providing a frequency limit of 3.75 Ghz, as determined by the Nyquist sampling theorem. However, the incident pulse bandwidth is less than 1 Ghz, hence the modes are presented only within this bandwidth. The string was excited from incident angles of 0, 25, 50, and 75 degrees. Figures 16 and 17 show results of a 256 point FFT of the time-domain data for the same segment in each figure. These figures show results obtained on segment number 22 and 6, respectively. In both cases the modes excited for different incident angles appear to be the same. Note that for the 0 degree incident angle (solid line), only the even modes are excited.

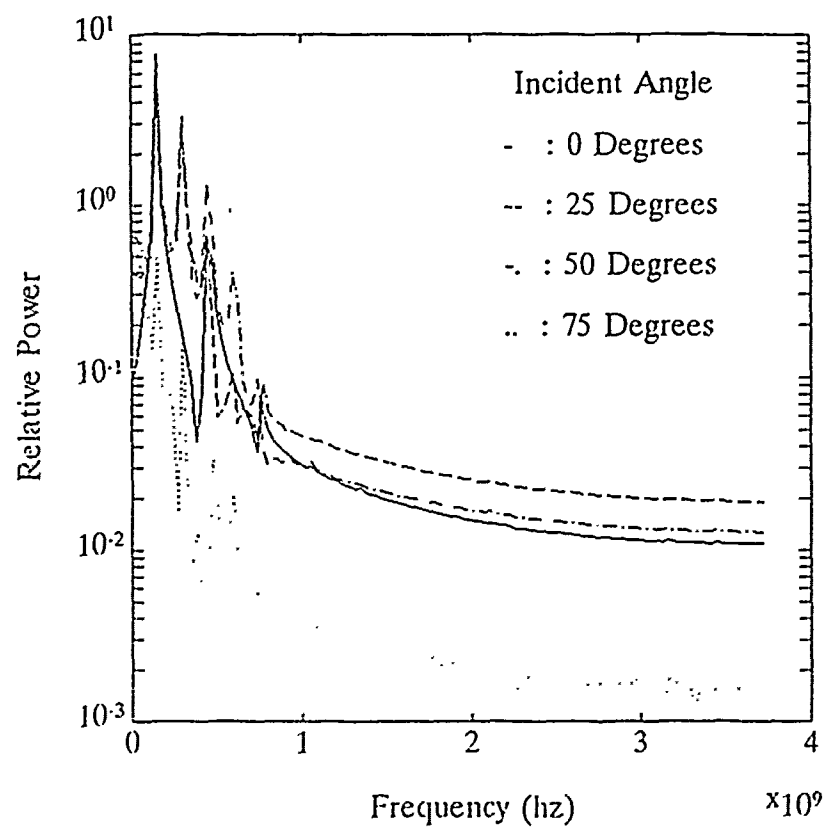


Figure 16. Modes on Segment 22

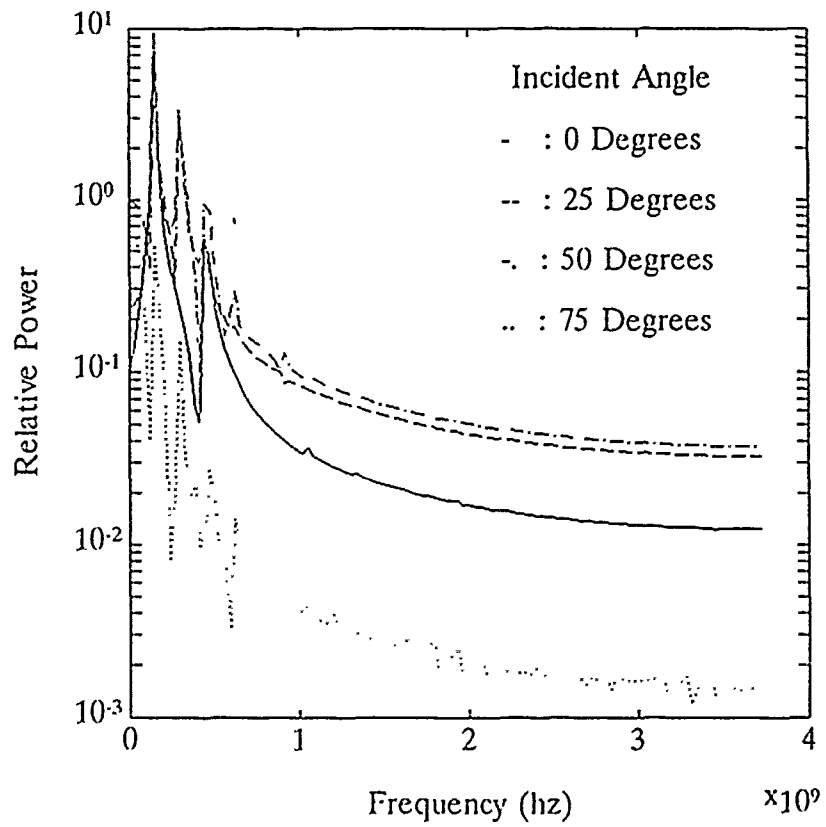


Figure 17. Modes on Segment 6

## IV. THE DISCRETE ARMA MODEL

### A. INTRODUCTION

Based on the theory of natural resonance scattering, a radar target can be considered as a Linear Time-Invariant (LTI) system. There are several ways of describing LTI systems. A linear system can be described by its impulse response, by means of linear difference equations, a system diagram or by the system transfer function with poles and zeros. The system transfer function model is extensively used to present natural resonance modes in transient scattering research. As previously mentioned, these modes are functions of the scatterer geometry and composition, and are independent of the incident excitation. A finite subset of the scatterer poles can possibly be used to represent the scatterer in the process of discrimination.

An alternative linear system model may be used to describe a scatterer in order to find its natural modes in a relatively simple way. This new approach describes a system by means of difference equations. Different scatterers, which are considered LTI systems, may be described by means of linear constant-coefficient difference equations. Once such a model has been set up for a specific scatterer, the natural modes can be directly determined by the coefficients of the differential equation.

In this work such a model has been set up for the late-time response of a vibrating string with forcing function. An alternate physical problem, which fits the mathematical model, is an illuminated TEM mode transmission line with either open

or shorted ends. In the equivalent electromagnetic case the late-time starts after the incident field has completed its illumination of the target, and is completely described using a weighted expansion of complex natural modes. During this period the scatterer acts as a recursive system, generating the natural resonance modes. The output of this system depends only on previous values of the output. This type of system can be described by an auto-regressive moving-average (ARMA) model. The coefficients for the recursive terms are constant since the feedback mechanisms on the scatterer are constant and time-independent. Moreover, the ARMA model which describes the system has the same recursive coefficients for all spatial points, as expected.

Two cases are considered: lossless and lossy . The analytical solution and the numerical solution for the natural modes in both cases are presented including comparisons with computed results. Development of the ARMA model for each case is then presented. Demonstrations of these developments are included through examples for both the lossless and lossy cases.

A variety of methods are currently used to estimate ARMA parameters. These methods have been used to estimate poles of scatterers by applying them to given data obtained by measuring the backscattering signal. In this work only the basic version of the Prony's method is applied to data obtained by the numerical solution described in Chapter III. The objective was to verify the development of the ARMA model. Results of the ARMA model are compared with results obtained using the Prony's method for pole estimation [Ref. 13].

## B. THE PROBLEM

The problems of transient electromagnetic scattering or the equivalent problem of acoustic scattering may be treated in the sampled signal case by considering the scatterer as a linear system whose input and output satisfy a linear constant-coefficient difference equation of the form

$$y(n) = \sum_{k=1}^N a_k y(n-k) + \sum_{k=0}^L b_k x(n-k). \quad (21)$$

For transient electromagnetic scattering, it is assumed that no surface current is on the scatterer before the scatterer is excited by the incident field, while the scatterer is initially at rest in the acoustic case. Therefore, the system may be considered casual, linear, and time-invariant. The  $a$ 's and the  $b$ 's in this case are real constants and the difference equation in Eq. (21) can be used to compute the output recursively [Ref. 6]. Considering the late-time case, the input  $x(n)$  is zero for  $n > n_0$ , where the discrete time  $n_0$  corresponds to  $T_0$  in the analog case. This is the time at which the incident field has completed its illumination of the scatterer. Hence, the difference equation for the late-time has the form

$$y(n) = \sum_{k=1}^N a_k y(n-k), \quad n > n_0. \quad (22)$$

Equation (22) describes the system model for the late-time where the unknowns are the coefficients  $a_1, a_2, \dots, a_N$ , and the number of delays  $N$ . Figure 18 shows the form of the system diagram, which serves as a graphical way of representing the same information contained in the difference equation (22). Equation (22) is referred to

as the homogeneous part of the general form of an Nth-order linear constant-coefficient difference described by Eq. (21) with  $a_0=1$ .

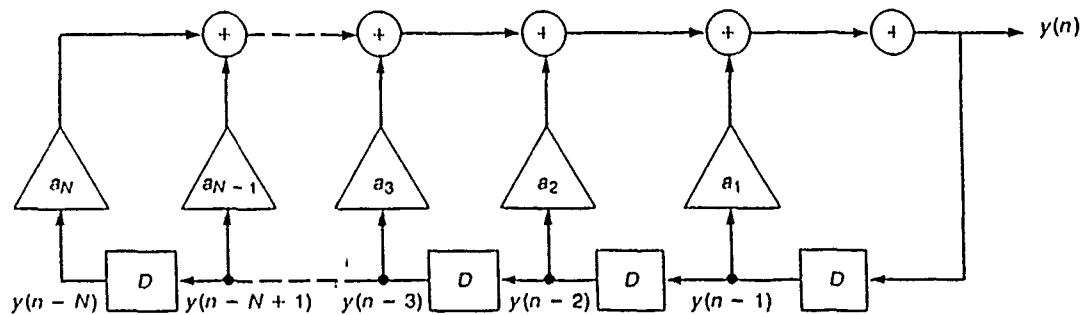


Figure 18. Realization of the General Model [After Ref. 5]

The homogeneous equation (22) has a family of solutions of the form

$$y(n) = \sum_{m=1}^N A_m z_m^n, \quad (23)$$

where  $z_m$  are complex numbers. A unique solution requires a set of  $N$  auxiliary conditions since there are  $N$  undetermined coefficients. Substituting Eq. (23) into Eq. (22), the complex numbers  $z_m$  must be roots of the polynomial

$$\sum_{k=0}^N a_k z^{-k} = 0, \quad (24)$$

assuming that all  $N$  roots of the polynomial in Eq. (24) are distinct. Based on the theory of natural resonance scattering, these roots are the poles in the  $z$ -transform



as the homogeneous part of the general form of an Nth-order linear constant-coefficient difference described by Eq. (21) with  $a_0=1$ .

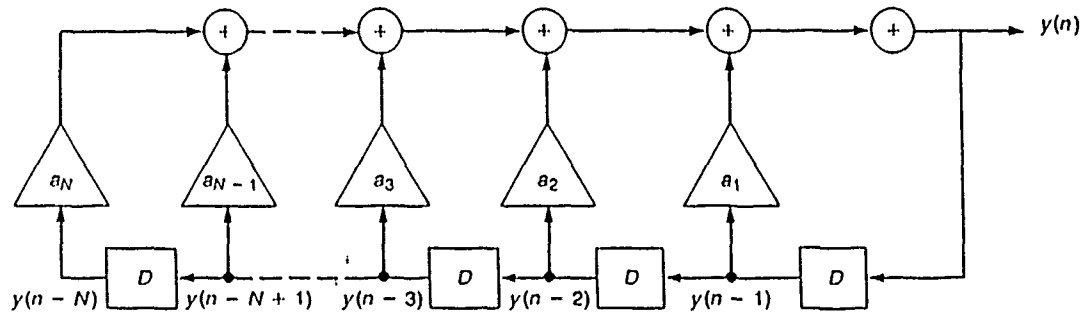


Figure 18. Realization of the General Model [After Ref. 5]

The homogeneous equation (22) has a family of solutions of the form

$$y(n) = \sum_{m=1}^N A_m z_m^n, \quad (23)$$

where  $z_m$  are complex numbers. A unique solution requires a set of  $N$  auxiliary conditions since there are  $N$  undetermined coefficients. Substituting Eq. (23) into Eq. (22), the complex numbers  $z_m$  must be roots of the polynomial

$$\sum_{k=0}^N a_k z^{-k} = 0, \quad (24)$$

assuming that all  $N$  roots of the polynomial in Eq. (24) are distinct. Based on the theory of natural resonance scattering, these roots are the poles in the  $z$ -transform

x and t may be separated by substituting the solution (26) into the PDE (25) to obtain the eigenvalue problem

$$\frac{\partial^2 u_n(x)}{\partial x^2} - \frac{s_n^2}{c^2} u_n(x) = 0, \quad (27)$$

with the boundary conditions  $u_n(0) = u_n(L) = 0$ . The general solution for the eigenvalue problem has the form

$$u_n(x) = c_1 e^{s_n x/c} + c_2 e^{-s_n x/c}. \quad (28)$$

The boundary conditions are applied to obtain the solutions for  $s_n$  and the associated modes. For the lossless case  $s_n = j\omega_n$ , where  $\omega_n = n\pi c/L$  for  $n = \pm 1, \pm 2, \dots$ . Natural resonance modes have the form

$$U_n(x, t) = \sin\left(\frac{n\pi}{L}x\right) e^{j\omega_n t}. \quad (29)$$

The trivial solution is obtained for  $n=0$ . The solution for the initial value problem may be obtained by writing the final solution as a superposition of natural modes

$$U(x, t) = \sum_{n=-\infty}^{\infty} A_n U_n(x, t), \quad n \neq 0. \quad (30)$$

The constants  $A_n$  which are usually complex, can be found by applying the initial conditions and representing them by the appropriate Fourier series, then matching term by term.

An alternative way to find the natural mode expansion for the initial value problem is by using the fact that these modes appear in conjugate pairs for real initial values. In this case the solution can be represented by

$$U(x,t) = \sum_{n=1}^{\infty} c_n \sin\left(\frac{n\pi}{L}x\right) \cos(\omega_n t + \phi_n), \quad (31)$$

where  $U_n = U_n^*$ . The real coefficients  $c_n$  and the unknown phase  $\phi_n$  are determined by the initial conditions using Fourier series to represent the initial condition functions and matching term by term.

For the lossy case the solution represented by Eq. (26) may be applied,  $u_n(x) = \sin(n\pi x/L)$ , but a slightly different solution is obtained for the modes. This solution is substituted into the lossy wave equation which has the form

$$\frac{\partial^2 U}{\partial x^2} - \frac{1}{c^2} \frac{\partial^2 U}{\partial t^2} - \xi \frac{\partial U}{\partial t} = 0, \quad (32)$$

where  $\xi > 0$  is the coefficient for the loss term. The eigenvalue problem for the spatial variable  $x$  has a different form, yielding a complex set of solutions for  $s_n$ . Substituting Eq. (26) into Eq. (32) to separate the variables  $x$  and  $t$ , the following equation is obtained for the variable  $x$ :

$$\frac{\partial^2 u_n(x)}{\partial x^2} - \left(\frac{s_n^2}{c^2} + \xi s_n\right) u_n(x) = 0, \quad s_n = \sigma_n + j\omega_n. \quad (33)$$

The solution for  $s_n$  is found as roots of the quadratic equation

$$s_n^2 + \xi c^2 s_n + \left(\frac{n\pi c}{L}\right)^2 = 0. \quad (34)$$

#### D. NUMERICAL SOLUTION FOR RESONANCE MODES: LOSSLESS CASE

The solution for the natural resonance modes involves the finite difference discrete form of the wave equation, using the star operator. Figure 19 shows the space-time discrete domain as applied to this development. The finite difference approximation results in a discrete *equation of evolution* which may be written for the lossless case in the following form

$$\bar{U}(k) = \underline{A} \cdot \bar{U}(k-1) - \bar{U}(k-2), \quad (35)$$

where

$$\bar{U}(k) = \begin{bmatrix} u(x_1, t_k) \\ u(x_2, t_k) \\ \vdots \\ u(x_M, t_k) \end{bmatrix}, \quad \underline{A} = \begin{bmatrix} 0 & 1 & 0 & \dots & 0 \\ 1 & 0 & 1 & 0 & 0 \\ 0 & \ddots & \ddots & \ddots & 0 \\ 0 & 0 & 1 & 0 & 1 \\ 0 & \dots & 0 & 1 & 0 \end{bmatrix}.$$

The vector  $U(k)$  is composed of unknown nodal values at the  $k$ -th time step and  $\underline{A}$  is an  $M \times M$  sparse matrix with ones along the two diagonals adjacent to the primary diagonal, regardless of size. The number of unknown nodal values is  $M$  which is

related to the number of segments by  $M=N'-1$ , where  $N'$  is the number of segments. The discrete form of the natural mode solution has the separable form

$$\bar{u}_n(k) = \bar{U}_n Z_n^k, \quad Z_n^k = e^{s_n k \Delta t} = e^{s_n t_k}, \quad (36)$$

where  $\bar{U}_n$  is a constant in  $k$ , and  $s_n = j\omega_n$  in the lossless case.

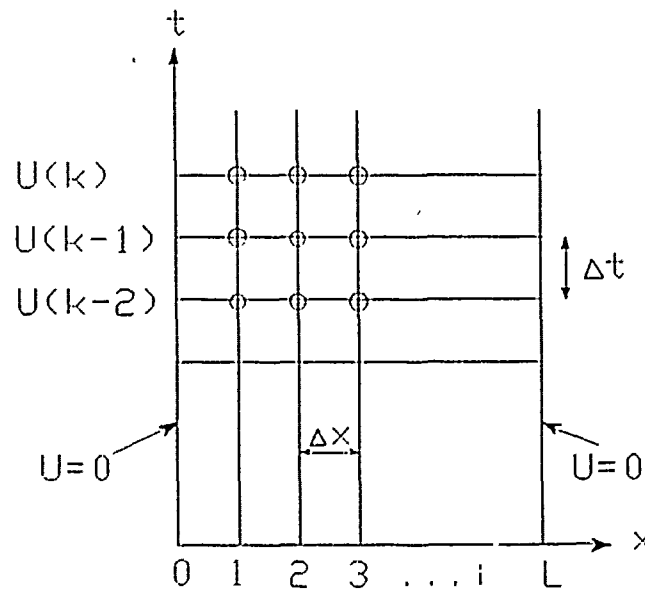


Figure 19. Space-Time Discretization for Mode Solution

Both  $u_n$  and  $Z_n$  should have acceptable values to solve Eq. (35). The solution for the natural modes may be obtained by substituting the solution in Eq. (36) into Eq. (35) to yield the following eigenvalue problem

$$A \cdot \bar{U}_n = (Z_n + Z_n^{-1}) \bar{U}_n = \lambda_n \bar{U}_n. \quad (37)$$

Equation (37) represents M linearly-independent equations for the M unknown eigenvalues  $\lambda_n$ . After solving Eq. (37) for the eigenvalues, the modes can be solved by the relation between  $Z_n$  and  $\lambda_n$ , via Eq. (37), as

$$Z_n + Z_n^{-1} = \lambda_n. \quad (38)$$

Equation (38) solves the natural modes. The number of modes is 2M since for every value of  $\lambda_n$  there are two solutions for the  $Z_n$  which are conjugate values. This can be explained by the fact that in the finite difference equation (35) there are 2M degrees of freedom since there are M unknowns, and each unknown requires two previous values. From this, it is concluded that 2M coefficients are expected to appear in the ARMA model. In terms of number of segments, the number of coefficients in the ARMA model is given by  $N=2(N'-1)$ , where  $N'$  is the number of segments.

The initial condition solution may be obtained by a superposition of the modes as

$$\bar{U}(k) = \sum_{n=1}^N A_n \bar{U}_n(k), \quad (39)$$

where  $N$  is the number of modes. The  $A_n$  terms are excitation dependent amplitudes and  $u_n(k)$  are excitation independent modes. There must be at least  $N=2M$  modes to allow the superposition (39) to be complete for any given initial conditions.

#### E. NUMERICAL SOLUTION FOR RESONANCE MODES: LOSSY CASE

The same solution procedure followed in the lossless case is applied to the lossy case. The finite difference equation may be written as

$$\bar{U}(k) = c_1 \underline{A} \cdot \bar{U}(k-1) - c_2 \bar{U}(k-2), \quad (40)$$

where  $c_1 = 2/(2 + A, c\xi \Delta x)$ ,  $c_2 = -c_1 + (c\xi \Delta x)/(2 + c\xi \Delta x)$ , and both  $\underline{A}$  and  $\bar{U}(k)$  have the same form as for the lossless case. Note that for the lossless case ( $\xi=0$ )  $c_1=1$  and  $c_2=-1$ . The same solution (36) is applied with  $s_n = \sigma_n + j\omega_n$ . By substituting the solution (36) into the PDE (40) and separating the variables, the following eigenvalue problem is obtained

$$c_1 \underline{A} \bar{U}_n = (Z_n + c_2 Z_n^{-1}) \bar{U}_n = \lambda_n \bar{U}_n. \quad (41)$$

Equation (41) represents  $M$  linearly-independent equations for  $M$  unknown eigenvalues. Solving Eq. (41) for the eigenvalues, the modes can be obtained by using the relation between  $\lambda_n$  and  $Z_n$  in Eq. (41) as

$$Z_n + c_2 Z_n^{-1} = \lambda_n. \quad (42)$$

The initial value problem may be solved by a superposition of the natural modes as in the lossless case, with  $N=2M$  modes to allow the superposition (39) to be completed for any given initial conditions.

#### F. ARMA MODEL DEVELOPMENT

The numerical solution shows that the modes are spatially-independent, i.e. all nodes have the same  $Z_n$ . Hence the ARMA model may have the following form

$$\bar{U}(k) = \sum_{m=1}^{N=2M} a_m \bar{U}(k-m), \quad (43)$$

where the  $a_m$ 's are the same for all spatial nodes, even those next to the boundaries, and  $\bar{U}(k)$  is the superposition of all  $U_n \cdot Z_n^k$ , for  $n \in [-M, M]$ . Note that the number of the coefficients is  $N=2M$ , where  $M$  is the number of spatial nodes along the string excluding those on the boundaries. The unknown coefficients can be determined by applying the z-transform to the recursion equation (43), which yields

$$\bar{U}_n Z_n^k = \sum_{m=1}^N a_m \bar{U}_n Z_n^{k-m}. \quad (44)$$

Equation (44) may be written for the coefficients in the form

$$Z_n^N = \sum_{m=1}^N a_m Z_n^{N-m}, \quad (45)$$



or in the form

$$Z_n^N - a_1 Z_n^{N-1} - a_2 Z_n^{N-2} - \dots - a_{N-1} Z_n - a_N = 0. \quad (46)$$

Factoring the left hand side of Eq. (46) into first-order terms gives

$$(Z-Z_1)(Z-Z_{-1})(Z-Z_2)(Z-Z_{-2}) \dots (Z-Z_M)(Z-Z_{-M}) \quad (47)$$

where  $Z_n$  are the poles and  $Z_n = Z_{-n}^*$ . The last step is to use the results of the natural modes in Eq. (47) generating the polynomial and comparing term by term to Eq. (46) to find the values of the coefficients.

The validation of the ARMA model can be obtained by showing that Eq. (43) can be derived directly from the equation of evolution (35) by working backwards. This point is further demonstrated using an example for the lossless case.

#### G. VALIDATION EXAMPLE: LOSSLESS CASE

Consider the case of  $N'=4$  segments of an undamped string. The number of unknowns is  $M=N'-1=3$ . The vector of the unknown nodal values at the  $k$ -th time step has the form

$$\bar{U}(k) = \begin{bmatrix} u(x_1, t_k) \\ u(x_2, t_k) \\ u(x_3, t_k) \end{bmatrix}.$$

The equation of evolution in this case has the form

$$\bar{U}(k) = \underline{A} \cdot \bar{U}(k-1) - \bar{U}(k-2), \quad (48)$$

with the matrix

$$\underline{A} = \begin{bmatrix} 0 & 1 & 0 \\ 1 & 0 & 1 \\ 0 & 1 & 0 \end{bmatrix}.$$

The number of discrete natural modes is  $N=2M=6$ . The eigenvalue problem with the form of Eq. (37) is obtained by substituting the separable form (36) into the equation of evolution (48). The eigenvalue problem has the following form after rearranging the equation

$$\underline{A} \cdot \bar{U}_n = (Z_n + Z_n^{-1}) \bar{U}_n = \lambda_n \bar{U}_n. \quad (49)$$

Substituting  $\underline{A}$  and solving for the eigenvalues gives three solutions:  $\lambda_n=0$ , and  $\lambda_n = \pm\sqrt{2}$ . The solution for the modes is obtained via

$$Z_n + Z_n^{-1} = \lambda_n \quad \lambda_n = 0, \sqrt{2}, -\sqrt{2}. \quad (50)$$

The solution has six modes:  $Z_n = e^{\pm j\pi/2}, e^{\pm j\pi/4}, e^{\pm j3\pi/4}$ . Figure 20 shows the six poles in the  $z$ -plane. The poles are on the unit circle since this system is lossless. Since  $Z_n = e^{j\theta}$ , where  $\theta = \omega_n \Delta t$ , the modes are the same as in the exact case  $\omega_n = n\pi/4\Delta t = n\pi c/L$ .

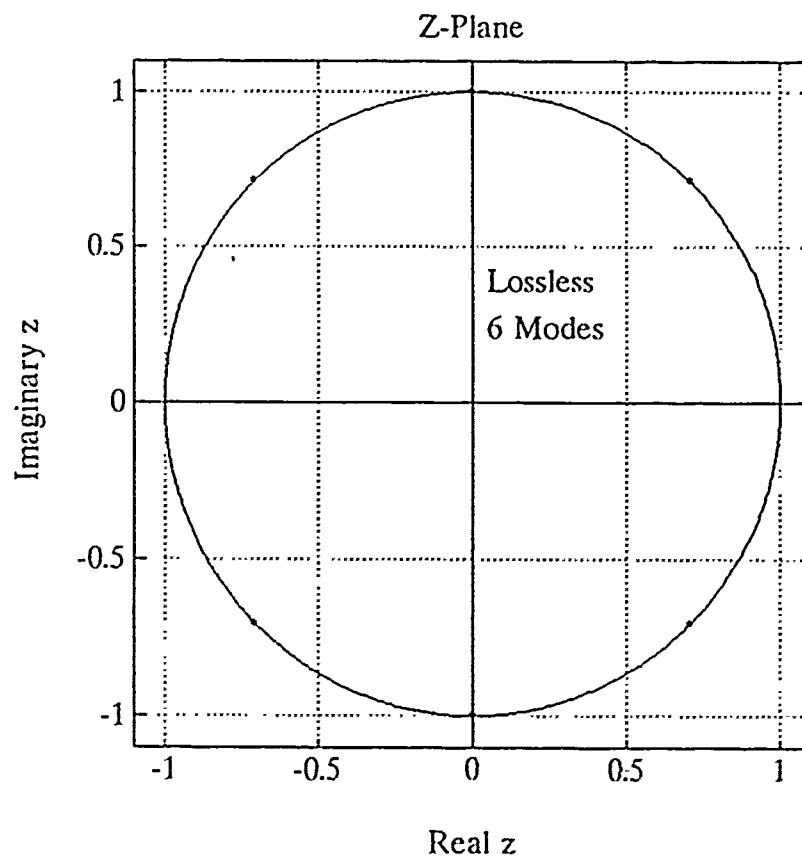


Figure 20. Modes of 4 Segment Undamped String

The ARMA model has the form

$$\bar{U}(k) = \sum_{m=1}^6 a_m \bar{U}(k-m). \quad (51)$$

The z-transform of Eq. (51) is

$$Z_n^N = \sum_{m=1}^6 a_m Z_n^{(N-m)}. \quad (52)$$

The coefficients  $a_m$  can be found by factoring

$$(Z-Z_1)(Z-Z_1^*)(Z-Z_2)(Z-Z_2^*)(Z-Z_3)(Z-Z_3^*), \quad (53)$$

with the known solutions for the  $Z_n$ . The polynomial obtained by this procedure is

$$Z^6 + Z^4 + Z^2 + 1, \quad (54)$$

which gives the coefficients:  $a_1=0$ ,  $a_2=-1$ ,  $a_3=0$ ,  $a_4=-1$ ,  $a_5=0$ , and  $a_6=-1$ . The ARMA model for this case has the form

$$\bar{U}(k) = -\bar{U}(k-2) - \bar{U}(k-4) - \bar{U}(k-6). \quad (55)$$

Verification of the ARMA model may be done by using the finite-difference equation of evolution (48) to find the coefficients in Eq. (55). The procedure is to use Eq. (48) to write  $\bar{U}(k-1)$ ,  $\bar{U}(k-3)$ , and  $\bar{U}(k-5)$  to finally obtain the form in (55). This is shown in Appendix B.

In a case of a 5-segment string, there are 4 unknowns for each time step, and therefore 8 modes. The poles obtained in this case are  $Z_n = e^{\pm j\pi/5}$ ,  $e^{\pm j2\pi/5}$ ,  $e^{\pm j3\pi/5}$ , and  $e^{\pm j4\pi/5}$ . These poles are shown in Fig. (21) on the unit circle of the z-plane.

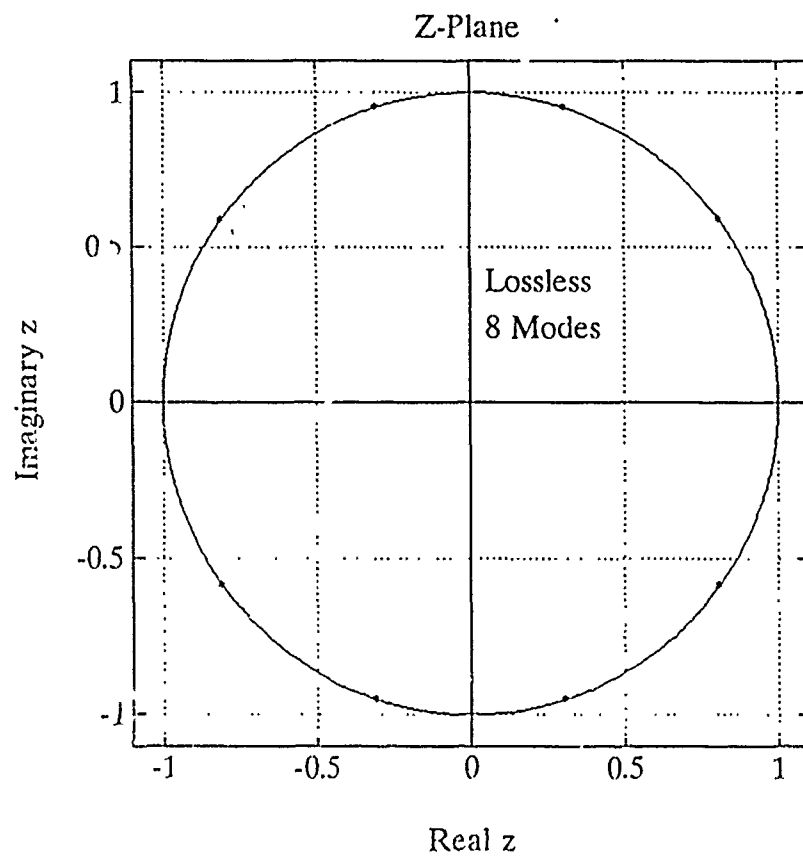


Figure 21. Modes of 5 Segment Undamped String

## H. VALIDATION EXAMPLE: LOSSY CASE

Consider the case of  $N'=4$  segments on a damped string. The number of unknowns is  $M=N'-1=3$ . The vector of the unknown nodal values at the  $k$ -th time step has the form of that in the example of the lossless case. The equation of evolution in this case has the form

$$\bar{U}(k) = c_1 \underline{A} \bar{U}(k-1) - c_2 \bar{U}(k-2), \quad (56)$$

where

$$c_1 = \frac{2}{2+c\xi\Delta x}, \quad c_2 = \frac{c\xi\Delta x}{2+c\xi\Delta x} - c_1.$$

The same matrix  $\underline{A}$  as in Eq. (48) is applicable in this case. The number of discrete natural modes is  $N=2M=6$ . The eigenvalue problem with the form (37) is obtained by substituting the separable form (36) into the equation of evolution (56). The eigenvalue problem has the same form as in the lossless case. Substituting  $\underline{A}$  and solving for the eigenvalues gives three solutions:  $\lambda_n=0$ , and  $\lambda_n=\pm c_1\sqrt{2}$ . The solution for the modes is obtained via

$$Z_n + c_2 Z_n^{-1} = \lambda_n \quad \lambda_n=0, \quad c_1\sqrt{2}, \quad -c_1\sqrt{2}. \quad (57)$$

The solution has six poles,

$$Z_n = \sqrt{|c_2|} e^{\pm j\frac{\pi}{2}}, \quad Z_n = \frac{\pm\sqrt{2}c_1 \pm \sqrt{2c_1^2 + 4c_2}}{2}.$$

Figure 22 shows these six poles in the z-plane. The poles are inside the unit circle and on a circle representing equal loss for all modes. In the electromagnetic case, as the frequency increases the higher frequency modes have more loss.

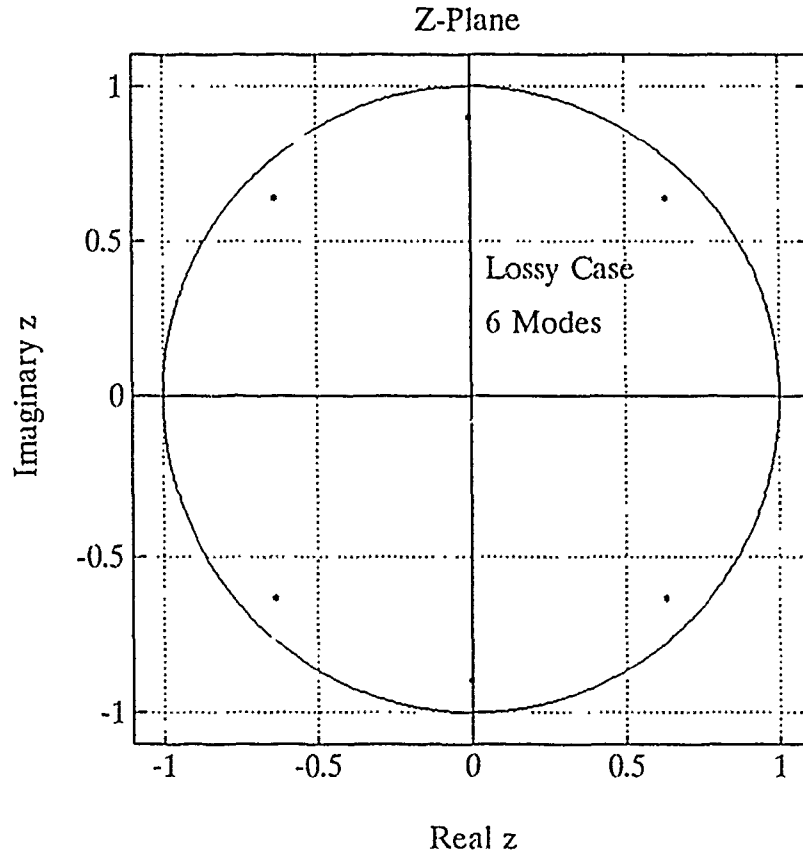


Figure 22. Modes of 4 Segment Damped String

The ARMA model has the form

$$\bar{U}(k) = \sum_{m=1}^6 a_m \bar{U}(k-m). \quad (58)$$

The same procedure used to find the coefficients for the lossless case is applied in the lossy case. The coefficients  $a_m$  can be found by factoring the solutions for  $Z_n$ .

The coefficients in this case are:  $a_1=0$ ,  $a_2=3c_2+2c_1^2$ ,  $a_3=0$ ,  $a_4=-3c_2^2+2c_2c_1^2$ ,  $a_5=0$ , and  $a_6=c_2^3$ . Note that the non-zero  $a$ 's are negative numbers with decreasing absolute values as their index increases. The ARMA model in this case has the form

$$\bar{U}(k) = (3c_2+2c_1^2) \bar{U}(k-2) - (3c_2^2+2c_2c_1^2) \bar{U}(k-4) + c_2^3 \bar{U}(k-6). \quad (59)$$

Checking the coefficients by using  $c_1=1$ , and  $c_2=-1$  yields the same coefficients obtained in the lossless case.

## I. COMPUTED RESULTS

The objective of this part of the work was to obtain additional verification for the ARMA model. The idea was to apply an algorithm which can estimate ARMA model coefficients to the time domain data generated by the computer program TH7.FOR. There are several methods available to estimate these parameters. Among them is the Prony's method [Ref. 13]. The Prony's method implemented via a computer program entitled TEST.M. A source listing is given in Appendix C. The program implements the following procedure for each segment on the wire.

Using the time-domain results of a given segment, the following  $M \times M$  matrix and vector are generated

$$P = \begin{bmatrix} u(t-1) & u(t-2) & \dots & u(t-M) \\ u(t-2) & u(t-3) & \dots & u(t-M-1) \\ \vdots & \vdots & \dots & \vdots \\ u(t-M) & u(t-M-1) & \dots & u(t-2M-1) \end{bmatrix}, \quad V = \begin{bmatrix} u(t) \\ u(t-1) \\ \vdots \\ u(t-M+1) \end{bmatrix},$$



where  $M$  is the number of coefficients, and  $t$  is the time step at which the ARMA model is applied. The time-step  $t$  should be "late" enough so the time step  $t-2M-1$  is in the late-time portion of the time-domain solution,  $u(t)$  of the given segment. The vector  $\bar{a}$  is composed of the coefficients  $a_1, a_2, \dots, a_M$ . The  $a_m$ 's coefficients are computed by

$$\bar{a} = P^{-1} \cdot V, \quad (60)$$

where  $P^{-1}$  is the inverse matrix of  $P$ . This method was applied to various cases. The results show that the coefficients are the same for all segments. The coefficients are also the same for any time-step  $t$  in the late-time,  $t-2M-1 > n_0$ , where  $n_0$  is the initial time-step of the late-time portion of the system response. For all lossless cases the results show coefficients with the form  $a_1=0, a_2=-1, a_3=0, a_4=-1, \dots, a_M=-1$ . In all lossy cases the results are  $a_i=0$  for odd  $i$ , and decreasing absolute values of negative numbers  $a_i$ , for even  $i$ . In some cases the results were different from segment to segment. In those cases where the results produced segment-dependent coefficients the frequency response showed that not all of the modes were excited. A representative result is shown in Fig. 23. In this case, the damped string was subdivided into 11 segments, hence the number of modes is 20. The same coefficients were obtained for all segments, for various incident angles, and at each time-step in the late-time.

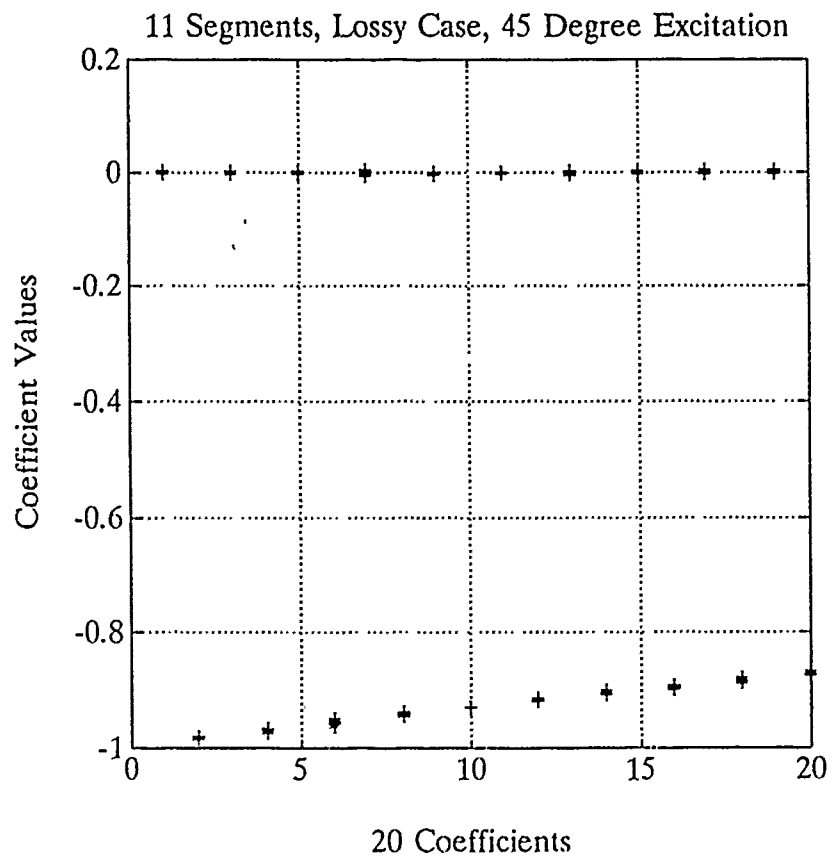


Figure 23. ARMA Model Coefficients of Damped String

## VI. CONCLUSIONS

The solution of electromagnetic natural resonance modes by means of finite difference equations promises to be useful and effective. The ability to construct discrete ARMA type models of complex scatterers may be applicable to estimating their electromagnetic signature. In this thesis a simple ARMA model for the case of the one-dimensional wave equation was investigated in order to examine this new approach. Complex three-dimensional scattering structures can be treated using a space-time finite-difference approach which is an extension to that investigated herein. The ARMA model was constructed for the late-time response when the scatterer acts as a recursive LTI system. The process of constructing such a model included two main steps. First the scatterer should be presented in a discrete form. In this work the finite-difference approach was presented as well as the time-domain integral equation. The finite-difference approach is found to be convenient for the construction of the required model. The advantage of this method is in the locally-connected discrete form which can be effectively used in the next step. In the second step, an algorithm is constructed to explicitly present the natural modes. In this work, the algorithm is based upon the star operator obtained from the finite difference approach. It was shown that the star operator was used recursively to yield the ARMA model, with constant coefficients.

Results of this work have shown again, in the case of acoustic scattering, that natural resonance modes of a scatterer are spatial- and aspect-independent. The scatterer acts as a complete recursive system only in the late-time. Since the early-time is important because of practical considerations of signal to noise ratio, further work is required to extend the model to and to examine its complexity in the early-time. The computer program entitled TH7.FOR can be modified to help this investigation.

The electromagnetic thin-wire scattering case was formulated via the vector potential. However, the potential on the ends of the wire is unknown. Assuming homogeneous boundary conditions reduces the problem to that of a vibrating finite string with zero displacement at the ends. Extension to the electromagnetic case may be made by attempting to discretize the current on the wire using the EFIE. In the case of currents, the boundary conditions are zero.

A better approach is found by employing the finite-difference approach. In this method the spatial point current is given in terms of its "nearest-neighbor" currents yielding the applicable star operator. The ARMA model is constructed using the star operator.

## APPENDIX A. SPACE-TIME WAVE EQUATION PROGRAM

The program entitled TH7.FOR numerically solves the displacement of a finite string. The equation for the position  $U(x,t)$  obeys the wave equation including a term of loss

$$\frac{\partial^2 U(x,t)}{\partial x^2} - \frac{1}{c^2} \frac{\partial^2 U(x,t)}{\partial t^2} - R \frac{\partial U(x,t)}{\partial t} = f(x,t).$$

The program uses the finite-difference method, with central difference, to solve the partial differential equation (PDE). The string with length  $L$  meters is subdivided into  $N$  segments. The boundary conditions  $U(x=0,t)$  and  $U(x=L,t)$  are set to zero. The excitation is a Gaussian pulse with the form

$$f(x,t) = GA \cdot \exp^{-a_1 (t-t_{\max} - x \tan \theta)^2}.$$

The pulse width is set between "10%" points ( $T1$  in the program), where  $\theta$  is the incident angle. The time-delay to peak pulse impact is  $T2$ . The times  $T1$ ,  $T2$  and  $\theta$  can be defined in the program, along with the amplitude of the Gaussian pulse,  $GA$ . Both space and time intervals are defined as  $S$  and  $T$ , respectively.

```
c  VARIABLES DECLARATION
c
  INTEGER N,NNEXT,Th
  REAL L,S,GA,C1,R,A,B,P,D,U1,U2,Tmax,T1,T2,A2,A1,PL(403)
  REAL PI,Tht,T3
  CHARACTER*64 TITLE
```

DIMENSION U(103,403), F(103,403)

C

```
write(*,*)
write(*,*) PROGRAM TH7.FOR    COHEN YUVAL    MAY 1990 '
write(*,*)
write(*,*)          SPACE-TIME WAVE EQUATION PROGRAM
write(*,*)
write(*,*) The program solves numerically the displacement
write(*,*) of a finite string. The equation for  $U(x,t)$  is the
write(*,*) wave equation including a term of loss.
write(*,*) The program uses the "Finite Difference Method"
write(*,*) to solve the Partial Differential Equation (PDE)
write(*,*) The string with length L meter is subdivided into
write(*,*) N segments. The boundary conditions are
write(*,*)  $U(x,t)=U(L,t)=0$  and initial conditions  $U(x,0)=0$ 
write(*,*) and  $dU(x,0)/dt=0$ . The excitation is a gaussian
write(*,*) pulse:  $G=Ga*EXP(-a*(t-Tmax-x*tan(Theta))**2)$ 
write(*,*) The pulse width is set between "10%" points. The
write(*,*) incident angle is Theta. The space step is S and
write(*,*) the time step is T.
write(*,*)
write(*,*)          Ready to begin ?
write(*,*)
write(*,*)
write(*,*)
pause
```

C

C INITIALIZATION

C

```
WRITE(*,*)
WRITE(*,*) 'Enter number of your MONITOR Type'
WRITE(*,*) ' CGA ==> Enter 0 '
WRITE(*,*) ' EGA ==> Enter 1 '
READ (*,*) NS
WRITE(*,*)
WRITE(*,*) 'Enter number for "Form Feed" after plot'
WRITE(*,*) ' Enter 0 ==> NO FORMFEED (Laser)'
WRITE(*,*) ' Enter 1 ==> FORMFEED (Impact)'
WRITE(*,*)
READ (*,*) NFD
ILINE=2
Pi=3.14159
C0=2.9979E+8
Thi=0.0
Th=0
a1=(-1.0)*LOG(0.1)
WRITE(*,*)
WRITE(*,*) ' ENTER : String length in Meters'
WRITE(*,*)
READ(*,*) L
WRITE(*,*)
```

```

WRITE(*,*)
WRITE(*,*) ' ENTER : Gaussian pulse parameters'
WRITE(*,*) ' Enter : Amplitude GA'
WRITE(*,*)
READ(*,*) GA
WRITE(*,*)
WRITE(*,*)
WRITE(*,*)
T1=1e-9
T2=0.6*T1
c
CONTINUE
NNEXT=0
WRITE(*,*) ' ENTER number of segments N'
WRITE(*,*) ' (Any integer between 2 to 100)'
READ(*,*) N
WRITE(*,*)
S=L/N
c ' choose S/T=C '
T=S/C0
WRITE(*,*) ' How many TIME steps to compute ?'
WRITE(*,*) ' Enter Integer between 2 to 400'
WRITE(*,*)
READ(*,*) M
WRITE(*,*)
WRITE(*,*) ' Enter : coefficient R '
WRITE(*,*) ' ( R>0 or R=0 ) in 1E-10 Units'
WRITE(*,*) ' The case R=0 is LOSSLESS case.'
WRITE(*,*)
READ(*,*) R
R=R*1E-10
C1=C0*R*S
A=2/(2+C1)
P=(C1/(2+C1))-A
D=A*(S**2)*(-1.0)
IF(NNEXT.EQ.0) GO TO 8
c
5 CONTINUE
WRITE(*,*) ' Enter Pulse width in NSEC'
READ(*,*) T1
T1=T1*1E-9
WRITE(*,*) ' Enter Time delay in NSEC for Peak Pulse Impact'
READ(*,*) T2
T2=T2*1E-9
NNEXT=0
8 CONTINUE
Tmax=T1/2
a2=a1/(Tmax**2)
IF(T2.GT.Tmax) GO TO 9
WRITE(*,*) ' Time delay must be longer then half pulse width!'

```

```

WRITE(*,*) '          TRY AGAIN !!!'
GO TO 5
6 CONTINUE
7 CONTINUE
WRITE(*,*) ' Enter Incident Angle in DEGREE ( 0<=Theta=<90 )'
READ(*,*) Th
IF (Th .GT. 90 .or. Th .LT. 0) then
WRITE(*,*) ' TRY AGAIN !    0=< Theta <=90 '
GO TO 7
END IF
NNEXT=0
9 CONTINUE
c
c GENERATE BOUNDARY and INITIAL CONDITIONS
DO 300 j=1,M+2
DO 400 i=1,N+1
    U(i,j)=0.
400 CONTINUE
300 CONTINUE
c
c GENERATE GAUSSIAN PULSE EXCITATION E=G*EXP(-a*(t-Tmax)**2)
c PULSE WIDTH at *10%* POINTS.
c
    Tht=(Th/180.0)*Pi
    T3=T*tan(tht)
    DO 600 i=1,N
    DO 500 j=1,M+2
        F(i,j)=GA*exp((-1.0)*A2*((j-1)*T-T2-((i-1)*T3))**2)
500 CONTINUE
600 CONTINUE
    WRITE(*,*) ' Want to create file "f.mat" with driver data ?'
    WRITE(*,*) '          NO ==> Enter 0'
    WRITE(*,*) '          YES ==> Enter 1'
    READ(*,*) I
    IF (I .EQ. 0) GO TO 23
    OPEN(4,file='f.mat')
    DO 100 j=1,M+2
    DO 200 i=1,N
        WRITE(4,*) f(i,j)
200 CONTINUE
100 CONTINUE
    CLOSE (4)
23 CONTINUE
c
c DISPLACEMENT COMPUTATION : MARCHING FORWARD IN TIME
c
DO 700 j=3,M+2
    jj=j-2
    DO 800 i=2,N
        ii=i-1

```



```

      U1=A*(U(i+1,j-1)+U(i-1,j-1))
      U2=P*U(i,j-2)+D*F(ii,jj)
      U(i,j)=U1+U2
800  CONTINUE
700  CONTINUE
C
C  CREATE a DATA FILE for OUTPUT POST PROCESSING (matlab)
WRITE(*,*) ' Want to create file "U.mat" with displacement data ?'
WRITE(*,*) '          NO ==> Enter 0'
WRITE(*,*) '          YES ==> Enter 1'
READ(*,*) I
IF (I .EQ. 0) GO TO 24
OPEN(3,file='U.mat')
DO 710 j=2,M+2
DO 720 i=1,N+1
  WRITE(3,*) U(i,j)
720  CONTINUE
710  CONTINUE
  CLOSE (3)
C
C  OUTPUT
C
24  CONTINUE
  IF(NNEXT.EQ.0) GO TO 10
  2  CONTINUE
  WRITE(*,20) M
20  FORMAT(' Enter TIME in Time Step Units: [t=1,2...M=',I3,']')
  READ(*,*) J
  OPEN(2,FILE='X')
  WRITE(2,11) J,N,Th
11  FORMAT('Displacement at TIME t=',I3,' STEPS. ',I3,
  $' SEG., Theta=',I3)
  REWIND(2)
  READ(2,12) TITLE
12  FORMAT(A)
  REWIND(2)
  NPTS=N+1
  Xmin=0
  Xmax=N
  j=j+2
  DO 900 i=1 , N+1
    PL(i)=U(i,j)
900  CONTINUE
  CALL PLTSUB(title,npts,xmin,xmax,xmin,xmax,pl,ns,nfd,iline)
  GOTO 10
C
3  CONTINUE
  N1=N-1
  WRITE(*,21) N1
21  FORMAT(' Enter SEGMENT NUMBER: [1,2,...N-1=',I3,']')

```

```

      READ(*,*) i
      OPEN(2,FILE='X')
      WRITE(2,13) i,N,Th
13  FORMAT('DISPLACEMENT of SEGMENT #',I3,' ',I3,' SEG., Theta=',i3)
      REWIND(2)
      READ(2,14) TITLE
      REWIND(2)
14  FORMAT(A64)
      i=i+1
      NPTS=M
      Xmin=0
      Xmax=M
      DO 910 j=1,M+1
      PL(j)=U(i,j+1)
910  CONTINUE
      CALL PLTSUB(title,npts,xmin,xmax,xmin,xmax,pl,ns,nfd,iline)
      GOTO 10

C
  4  CONTINUE
      N1=N-1
      WRITE(*,22) N1
22  FORMAT(' Enter SEGMENT NUMBER: [1,2,...N-1=',I3,']')
      READ(*,*) i
      OPEN(2,FILE='X')
      WRITE(2,15) i,T11,T22,N,Th
15  FORMAT('Driver on Seg.:',i3,',Tpw=',F6.3,' ns,Td=',F6.3,
$' ns,N=',I3,',Theta=',i3)
      REWIND(2)
      READ(2,16) TITLE
      REWIND(2)
16  FORMAT(A64)
      NPTS=M
      Xmin=0
      Xmax=NPTS
      DO 920 j=1,NPTS
      PL(j)=F(i,j)
920  CONTINUE
      CALL PLTSUB(title,npts,xmin,xmax,xmin,xmax,pl,ns,nfd,iline)
10  CONTINUE
      WRITE(*,*)
      WRITE(*,*) ' SELECT Number for Results or Change data'
      WRITE(*,*) ' -----'
      WRITE(*,*) ' Change Data      AGAIN??          ==> 1'
      WRITE(*,*) ' Displacement on the wire at time t=.. ==> 2'
      WRITE(*,*) ' Displacement on Segment #..          ==> 3'
      WRITE(*,*) ' Pulse Excitation as Function of Time      ==> 4'
      WRITE(*,*) ' Change Pulse Excitation Timing              ==> 5'
      WRITE(*,*) ' Change Pulse Excitation Incident ANGLE      ==> 6'
      T11=T1*1E+9
      WRITE(*,*)

```

```

WRITE(*,17) T11
17 FORMAT ( '      Current Values are: Pulse width=',f6.3,' ns.')
   T22=T2*1E+9
   WRITE(*,18) T22
18 FORMAT ( '      Time Delay for Peak Pulse Impact=',F6.3,' ns.')
   WRITE(*,19) Th
19 FORMAT ( '      Incident Angle : Theta =',i3,' Degree.')
   WRITE(*,*)
   WRITE(*,*) '      Any Other Integer ==> END PROGRAM !!!'
   WRITE(*,*)
   READ(*,*) NNEXT
   IF(NNEXT.EQ.1) GO TO 1
   IF(NNEXT.EQ.2) GO TO 2
   IF(NNEXT.EQ.3) GO TO 3
   IF(NNEXT.EQ.4) GO TO 4
   IF(NNEXT.EQ.5) GO TO 5
   IF(NNEXT.EQ.6) GO TO 6
   STOP
   END

C
C
C SUBROUTINE PLTSUB(TITLE,NPTS,XMIN,XMAX,XS,XF,F,NS,NFD,ILINE)
C
C MS-FORTRAN Subroutine using "Grafmatic" Library Subroutines.
C Solid Line Using Portions of "PLOT" Program.
C Written by M.A. Morgan with Latest Update to EGA/CGA June 1989.
C
C Default Printer is "IBM Graphics" (e.g. Epson, Okidata, IBM)
C With Plot Rotated 90 degrees From the Vertical. "GrafPlus.Com"
C May be Run to Rotate Plot Upright on Paper and to Use a Variety
C of Impact Printers. "GrafLaser.Com" May be Run to Use a Laser
C Printer. See GrafPlus/Laser Manual From Jewell Technology.
C
C INPUT DATA FORMAT
C
C TITLE - 64 Character Header
C NPTS - # Data Points Is
C XMIN - Min X-Axis value
C XMAX - Max X-Axis value
C XS - Starting X value for F(1)
C XF - Finishing X value for F(N)
C F(N) - Input Data Array
C NS - Monitor: "0"= CGA, "1"= EGA
C NFD - "1" --> Form Feed After Plot Hardcopy (Impact)
C Any Other Integer --> No Form Feed (Laser)
C ILINE - "1" --> + + + Symbol Dot Plot
C Any Other Integer --> Solid Line Plot
C
C NOTE: The X-Axis Range Can Be Made Larger Than
C The Domain of the Plotted Function, F(x).

```

```

C           Otherwise, Make XS=XMIN and XF=XMAX.
C
CHARACTER*1 DUM,BELL,FEED
CHARACTER*64 TITLE,FNAME,HCOPY
REAL X(512),F(512)
INTEGER*2 N,JROW,JCOL,ISYM,ITYPE,NSCRN
INTEGER*2 CYAN,WHITE,YELLOW,RED,BLACK,BLUE,NTWO
INTEGER*2 JROW1,JROW2,JCOL1,JCOL2
BELL=CHAR(7)
FEED=CHAR(12)
WRITE(*,*) BELL
WHITE=7
CYAN=11
YELLOW=14
RED=12
BLACK=0
BLUE=1
NTWO=2
NSCRN = 6 + 10*NS
IF(NFD.EQ.1) OPEN(1,FILE='PRN')
N=NPTS
DX=(XF-XS)/(N-1.0)
FMIN=0.0
FMAX=0.0
DO 22 K=1,N
  X(K)=XS+(K-1.0)*DX
  IF(F(K).LT.FMIN) FMIN=F(K)
22 IF(F(K).GT.FMAX) FMAX=F(K)
  IF(FMIN.GT.0.0) FMIN=0.0
  IF(FMAX.LT.0.0) FMAX=0.0
C   Computing Scale Factors for Vertical Axis
  ABSMIN=ABS(FMIN)
  ABSMAX=ABS(FMAX)
  YBIG=AMAX1(ABSMIN,ABSMAX)
  NSCL=INT(LOG10(YBIG))
  IF (YBIG.LT.1.0) NSCL=NSCL-1
  YSCL=10.**NSCL
  FMIN=FMIN/YSCL
  FMAX=FMAX/YSCL
  ABSMIN=ABSMIN/YSCL
  ABSMAX=ABSMAX/YSCL
  DO 33 K=1,N
33 F(K)=F(K)/YSCL
C   Adaptive Scaling Algorithm 5/89
C   Setting Polarity of YMIN and YMAX
  YMIN=0.0
  YBIG=0.0
  IF(FMIN.EQ.0.0) GO TO 37
  DY=0.5
35 CONTINUE

```

```

IF(YMIN!.GE.4.0) DY=1.0
YMIN=YMIN+DY
IF(ABSMIN.GT.YMIN) GO TO 35
YBIG=YMIN
YMIN=YMIN*FMIN/ABSMIN
37 YMAX=0.0
IF(FMAX.EQ.0.0) GO TO 41
DY=0.5
39 CONTINUE
IF(YMAX.GE.4.0) DY=1.0
YMAX=YMAX+DY
IF(ABSMAX.GT.YMAX) GO TO 39
IF(YMAX.GT.YMIN) YBIG=YMAX
YMAX=YMAX*FMAX/ABSMAX
41 CONTINUE
C   Calling GRAFMATIC Routines and Plotting F
C   Solid Line Graph Default
ITYPE=1
ISYM=-2
NDOTS=0
C   + + + Line Graph If ILINE=1
IF(ILINE.NE.1) GO TO 45
ISYM=-1
ITYPE=0
45 CONTINUE
JROW1= 35+25*NS
JROW2= 170+120*NS
JCOL1= 110-10*NS
JCOL2= 540
CALL QSMODE(NSCRN)
CALL QPTXT(64,TITLE,YELLOW,16,24)
CALL QPLOT(JCOL1,JCOL2,JROW1,JROW2,XMIN,XMAX,YMIN,YMAX,XMIN,
1      0.,0,1.,1.5)
CALL QSETUP(NDOTS,CYAN,ISYM,CYAN)
XMAJOR=(XMAX-XMIN)/5.0
CALL QXAXIS(XMIN,XMAX,XMAJOR,1,1,2)
IF(YBIG.LE.4.0) YMAJOR=0.5
IF(YBIG.GE.5.0) YMAJOR=1.0
IF(YBIG.EQ.8.0) YMAJOR=2.0
IF(YBIG.EQ.9.0) YMAJOR=3.0
IF(YBIG.EQ.10.) YMAJOR=2.0
CALL QYAXIS(YMIN,YMAX,YMAJOR,1,1,1)
JROW=32+21*NS+(ABS(YMIN)/(ABS(YMAX)+ABS(YMIN)))*(135+95*NS)
JCOL=80-8*NS
CALL QGTXT(3,'0.0',WHITE,JCOL,JROW,0)
CALL QPTXT(1,'S',YELLOW,5,18)
CALL QPTXT(1,'c',YELLOW,5,17)
CALL QPTXT(1,'a',YELLOW,5,16)
CALL QPTXT(1,'I',YELLOW,5,15)
CALL QPTXT(1,'e',YELLOW,5,14)

```

```

CALL QPTXT(1,'X',YELLOW,5,12)
CALL QPTXT(2,'10',YELLOW,4,10)
CALL QPTXT(1,'*',YELLOW,5,9)
CALL QPTXT(1,'*',YELLOW,5,8)
CALL QCMOV(0,8)
WRITE(*,150) NSCL
CALL QTABL(ITYPE,N,X,F)
C   Hardcopy Query - Updated 5/11/89
HCOPY='Hardcopy --> Enter P or p'
CALL QPTXT(30,HCOPY,RED,25,1)
CALL QCMOV(55,1)
READ(*,100) DUM
HCOPY='
CALL QPTXT(40,HCOPY,BLACK,25,1)
IF(DUM.NE.'P' .AND. DUM.NE.'p') GO TO 48
CALL QPSCRN
IF(NFD.EQ.1) WRITE(1,160) FEED
48  CONTINUE
C   Exit to Blue Background on Screen - To Change This,
C   Replace 'BLUE' in Calls to QPREG and QOVSCN to That Desired.
CALL QSMODE(NTWO)
CALL QPREG(0,BLUE)
CALL QOVSCN(BLUE)
100 FORMAT(A)
120 FORMAT(I5)
130 FORMAT(E12.3)
150 FORMAT(4X,I3,\)
160  FORMAT(' ',A,\)
RETURN
END

```

## APPENDIX B. ARMA MODEL ALGORITHM

This Appendix presents the development of the ARMA model using the *equation of evolution* for the lossless case example given in Chapter IV.

Start with the equation of evolution of the following form for  $M=3$

$$\bar{U}(k) = \underline{A} \cdot \bar{U}(k-1) - \bar{U}(k-2), \quad (1)$$

with the symmetric matrix

$$\underline{A} = \begin{bmatrix} 0 & 1 & 0 \\ 1 & 0 & 1 \\ 0 & 1 & 0 \end{bmatrix}.$$

Using Eq. (1) to express  $U(k-1)$ , substituting into Eq. (1) yields the following

$$\bar{U}(k) = -\bar{U}(k-2) + \underline{A}^2 \cdot \bar{U}(k-2) - \underline{A} \cdot \bar{U}(k-3). \quad (2)$$

Using Eq. (1) to express  $U(k-2)$  and substituting into Eq. (2) yields the following

$$\bar{U}(k) = -\bar{U}(k-2) + \underline{A}^2 \cdot [\underline{A} \cdot \bar{U}(k-3) - \bar{U}(k-4)] - \underline{A} \cdot \bar{U}(k-3). \quad (3)$$

Rearranging Eq. (3) and using the fact that for  $M=3$   $\underline{A}^3 = 2\underline{A}$ , the following expression is obtained:

$$\bar{U}(k) = -\bar{U}(k-2) + \underline{A} \cdot \bar{U}(k-3) - \underline{A}^2 \bar{U}(k-4). \quad (4)$$

Using Eq. (1) to write  $U(k-3)$ , substituting in Eq. (4), and adding and subtracting  $U(k-4)$  yields

$$\bar{U}(k) = -\bar{U}(k-2) - \underline{A} \cdot \bar{U}(k-5) + \bar{U}(k-4) - \bar{U}(k-4). \quad (5)$$

Using Eq. (1) to write  $U(k-4)$  and substituting in Eq. (5) yields

$$\bar{U}(k) = -\bar{U}(k-2) - \bar{U}(k-4) - \bar{U}(k-6). \quad (6)$$

Equation (6) has the form of the ARMA model for  $M=3$  described in Chapter IV Section G.



## APPENDIX C. PRONY'S METHOD PROGRAM

The computer program entitled TEST.M implements the Prony's method to estimate ARMA model coefficients using time-domain data. The program, which is written using MATLAB codes, finds the coefficients by implementing the procedure described in Chapter IV, Section I. The matrix with the time-domain data should be defined in a MATLAB format, and stored in a file called X.MAT. The data may be generated by TH7.FOR, and translated into MATLAB format using "translate" in MATLAB. The output of the program plots the results of the coefficients for each segment data. The coefficients are stored in a matrix called c where each column contains the coefficients for each segment data. Plots of results may be obtained by using the information in matrix c.

```
% TEST.M program by Yuval Cohen June 1990
% The program implements the Prony's method on time-domain data
% estimating ARMA coefficients of the late-time solution of the
% space-time wave equation.
%
load x
input('Enter number of segments of the string N')
ns=ans;
input('Enter number of coefficients M=2(N-1)')
m=ans;
input('Enter the time-step t')
t=ans;
c=[];
for l=1:ns n=0;
y=[];
u=[];
for i=1:m
for j=1:m
```

```
y(i,j)=x(t-j-n,l);  
end  
n=n+1;  
end  
for i=1:m u(i)=x(t-i+1,l);  
end  
u=u';  
a=y\ u;  
c(:,l)=a;  
plot(a)  
end
```

## LIST OF REFERENCES

1. C. E. Baum, "On the singularity expansion method for the solution of electromagnetic interaction problems," AFWL Interaction Notes, Note 88, Dec. 1971.
2. Mains, R. H., and D. L. Moffat, "Complex natural resonances of an object in detection and discrimination," TR-3424-1, Ohio State University, Electroscience Laboratory, Columbus, OH, June 1974.
3. Morgan, M. A., "Singularity expansion representation for fields and currents in electromagnetic scattering," *IEEE Trans. Antennas Propagat.*, Vol. AP-32, 466-473, May 1984.
4. Morgan, M. A., "Scatterer discrimination based upon natural resonance annihilation," *J. of Electromagnetic Waves and Applications*, Vol. 2, No. 5/6, pp. 481-502, 1988.
5. R. D. Strum and D. E. Kirk, *Discrete Systems and Digital Signal Processing*, pp. 82-90, Addison Wesley, New York, 1988.
6. A. V. Oppenheim and R. W. Schaffer, *Discrete-Time Signal Processing*, pp. 33-35, Prentice Hall, New Jersey, 1989.
7. M. L. Van Blaricum and Mittra, R., "A technique for extracting the poles and residues of a system directly from its transient response," *IEEE Trans. Antennas Propagat.*, Vol. AP-23, 777, 1975.

8. Mittra, R., "Integral equations in transient scattering." in *Transient Electromagnetic Fields*, L. Felsen, Ed., Springer-Verlag, New York, 75-127, 1976.
9. A. J. Poggio and E. K. Miller, "Integral equation solution of three-dimensional scattering problems," in *Computer Techniques for Electromagnetics*, Mittra, R., eds., pp. 159-261, Pergamon Press, New York, 1973.
10. Sayre, E. P., and R. F. Harrington, "Time-domain radiation and scattering by thin-wires," *Applied Science Res.*, Vol. 26, 413-444, 1972.
11. R. Haberman, *Elementary Applied Partial Differential Equations*, pp. 434-489, Sec. ed., Prentice Hall, Englewood Cliffs, New Jersey, 1987.
12. G. D. Smith, *Numerical Solution of Partial Differential Equations: Finite Difference Methods*, Third ed., pp. 1-24, Clarendon Press, Oxford, 1985.
13. M. K. Steven, "Autoregressive spectral estimation: methods," in *Modern Spectral Estimation*, A. V. Oppenheim, ed., pp. 217-252, Prentice Hall, Englewood Cliffs, New Jersey, 1988.

### INITIAL DISTRIBUTION LIST

	No. of Copies
1. Defense Technical Information Center Cameron Station Alexandria, VA 22304-6145	2
2. Library, Code 52 Naval Postgraduate School Monterey, CA 93943-5002	2
3. Chairman Code EC Department of Electrical and Computer Engineering Naval Postgraduate School Monterey, CA 93943-5000	1
4. Professor Michael A. Morgan Code EC/Mw Department of Electrical and Computer Engineering Naval Postgraduate School Monterey, CA 93943-5000	3
5. Professor Richard W. Adler Code EC/Ab Department of Electrical and Computer Engineering Naval Postgraduate School Monterey, CA 93943-5000	1
6. Dr. John N. Entzminger Director, Tactical Technology Office Defense Advanced Research Projects Agency 1400 Wilson Blvd. Arlington, VA 22209	1

- |     |  |   |
|-----|--|---|
| 7.  | Dr. Arthur Jordan<br>Code 1114SE<br>Office of Naval Research<br>800 N. Quincy Street<br>Arlington, VA 22217                        | 1 |
| 8.  | Dr. Rabiner Madan<br>Code 1114SE<br>Office of Naval Research<br>800 N. Quincy Street<br>Arlington, VA 22217                        | 1 |
| 9.  | Naval Attache<br>Embassy of Israel<br>3514 International Drive, N. W.<br>Washington D. C. 20008                                    | 1 |
| 10. | Rear Admiral Ishai Haramati<br>C/O Naval Attache<br>Embassy of Israel<br>3514 International Drive, N. W.<br>Washington D. C. 20008 | 1 |
| 11. | Captain Meir Morag<br>C/O Naval Attache<br>Embassy of Israel<br>3514 International Drive, N. W.<br>Washington D. C. 20008          | 1 |
| 12. | CDR Rami Sharon<br>C/O Naval Attache<br>Embassy of Israel<br>3514 International Drive, N. W.<br>Washington D. C. 20008             | 1 |
| 13. | LCDR Yuval Cohen<br>C/O Naval Attache<br>Embassy of Israel<br>3514 International Drive, N. W.<br>Washington D. C. 20008            | 2 |